DOKUZ EYLÜL UNIVERSITY
GRADUATE SCHOOL OF NATURAL AND APPLIED SCIENCES

MECHATRONIC DESIGN OF 3 AXIS WELDING POSITIONER WITH 1500 KILOGRAM LOADING CAPACITY

by
Şirin ADA

June, 2017
İZMİR

MECHATRONIC DESIGN OF 3 AXIS WELDING POSITIONER WITH 1500 KILOGRAM LOADING CAPACITY

A Thesis Submitted to the
Graduate School of Natural and Applied Sciences of Dokuz Eylül University
In Partial Fullfillment of the Requirements for the Degree of Master of Science
in Mechatronics Engineering

by
Şirin ADA

June, 2017
İZMİR

M.Sc THESIS EXAMINATION RESULT FORM

We have read the thesis entitled **"MECHATRONIC DESIGN OF 3 AXIS WELDING POSITIONER WITH 1500 KG LOADING CAPACITY"** completed by **ŞİRİN ADA** under supervision of **PROF. DR. HİRA KARAGÜLLE** and we certify that in our opinion it is fully adequate, in scope and in quality, as a thesis for the degree of Master of Science.

Prof. Dr. HİRA KARAGÜLLE

Supervisor

Yrd. Doç. Dr. Erkin GEZGİN

(Jury Member)

Yrd. Doç. Dr. Aytaç GÖREN

(Jury Member)

Prof.Dr. Emine İlknur CÖCEN
Director
Graduate School of Natural and Applied Sciences

ACKNOWLEDGEMENTS

I would like to express my gratitude to my thesis consultant Prof. Dr. Hira KARAGÜLLE, for all his time and effort. His guidance and input at every stage of my work truly helped me navigate this endavor.

I would also thank Asst. Prof. Murat AKDAĞ, Dr. Şahin YAVUZ and my friend Mert İLMAN for their intellectual inputs.

Finally, I would like to thank my parents and my sister who have supported me all the way since the begining of my studies. Their love gave me forces to make this work.

Şirin ADA

MECHATRONIC DESIGN OF 3 AXIS WELDING POSITIONER WITH 1500 KILOGRAM LOADING CAPACITY

ABSTRACT

Industrial automation and intelligent manifacturing systems have been widely used recently because of the emerging developments in embedded systems, motion control systems, actuators, sensors, microprocessors, industrial communication, computer aided design (CAD) and computer aided manifacturing (CAM) tools.

In this study, multi stage design approach is implemented to the mechatronic design of three axis welding positioner and also modular and systematic design criterias are considered. Also, different CAD and CAE tools are used during the design process. Kinematic - kinetic and dynamic structure of the system is analyzed. Also, performance task method is used for the trajectory planning and time history studies.

Keywords: Mechatronic design, dynamic modeling, trajectory planning

1500 KİLOGRAM YÜK KAPASİTELİ 3 EKSENLİ KONUMLANDIRICININ MEKATRONİK TASARIMI

ÖZ

Gömülü yazılım sistemleri, hareket kontrol sistemleri, eyleyiciler, sensörler, mikroişlemciler, endüstriyel haberleşme, bilgisayar destekli tasarım ve bilgisayar destekli üretim sistemlerindeki gelişmeler nedeniyle, endüstriyel otomasyon ve akıllı makine imalat ve üretim sistemleri son zamanlarda yaygın kullanım alanı bulmuştur.

Bu çalışmada, 3 eksenli konumlandırıcının mekatronik tasarımı çok basamaklı tasarım süreci olarak ele alınmış olup modüler ve sistematik tasarım yaklaşımı geliştirilmiştir. Tasarım sürecinde farklı CAD ve CAE tasarım ve analiz araçları kullanılmıştır. Sistemin kinematik, kinetik ve dinamik yapısı incelenmiştir. Ayrıca, yörünge planlama çalışması için performans hareket metodu kullanılmıştır.

Anahtar kelimeler: Mekatronik tasarım, dinamik modelleme, yörünge planlama

CONTENTS

LIST OF FIGURES

Page

LIST OF TABLES

CHAPTER ONE
INTRODUCTION

Industrial automation and intelligent manifacturing systems have been widely used recently because of the emerging developments in embedded systems, motion control systems, actuators, sensors, microprocessors, industrial communication, computer aided design (CAD) and computer aided manifacturing (CAM) tools (Bingül & Küçük, 2015).

Robot is a programmable multifunctional machinery designed to perform multiple tasks. In other word, Robot is a closed loop computer controlled industrial manipulator. Also, Robotic science is comprised of applied mathematics, physics, control, mechanical, electrics and computer engineering disciplines (Bingül & Küçük, 2015).

Today, industrial robots are widely used in every stage of manifacturing. Industrial applications of robots are;

- Painting
- Arc Welding
- Piercing/Deburring
- Mounting
- Injection Moulding
- Laser Cutting
- Water Jet Cutting
- Machine Tending
- Measuring/Testing
- Material Handling
- Forging
- Education/Research

1.1 Robot Classification

Robots are classified into five groups because of their structural and design spesifications. These are;

- Link structure types
- Control methods
- Actuator types
- Precision and repeatibility
- Degrees of Freedom (DoF)

1.1.1 Link Structure Types

- Cartesian configuration
- Cylindrical configuration
- Scara configuration
- Articulated configuration
- Spherical configuration

Figure 1.1 Industrial robot for arc welding (ABB, 2016)

Figure1.2 Parallel robot for pick and place applications (Omron, 2016)

Figure 1.3 Scara robot for material handling applications (Omron, 2016)

Figure 1.4 Cartesian robot for material handling and manifacturing applications

1.1.2 Control Methods

- Pick and place
- Continous trajectory controlled

1.1.3 Actuator Types

- Electrical actuator
- Pneumatic actuator
- Hydraulic actuator

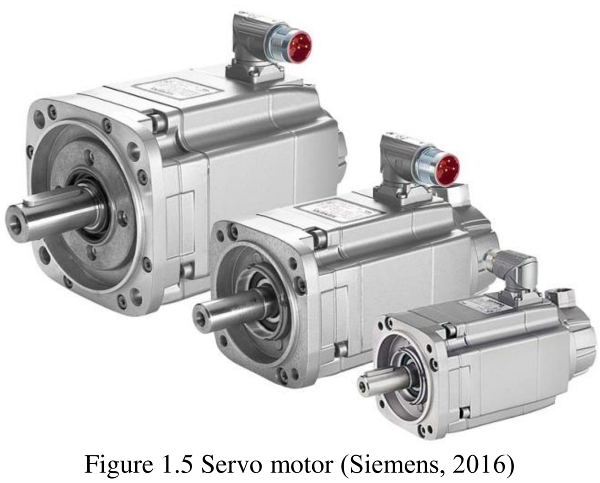

Figure 1.5 Servo motor (Siemens, 2016)

1.2 Considerations of Robotic Applications

- Dangerous and uncomfortable working environment
- Repeatable work tasks
- Heavy and dangerous material handling
- Different work tasks

1.3 Robots in Performing Welding Applications

Robots which are used in welding applications have capabilities in five, six or more axis motion as kinematic structure. Figure 1.6 shows industrial robots in automotive industry.

Figure 1.6 Robots in automotive industry (Kuka Robotics, 2016)

In arc welding applications, Robots are used with a welding positioner which move the workpiece from one position to another. For this reason, robot's motion flexibility is increased with additional positioner axis motions.

Robots have to perform up/down, left/right and angular motions of the welding gun and trace the welding path (welding seam) in welding direction. Hence six axis robots are widely used in robotic arc welding applications. These robot motion flexibility is identified by *workspace* which term is the sum of points of robot's end effector could reach. Figure 1.7 shows an industrial robot workspace.

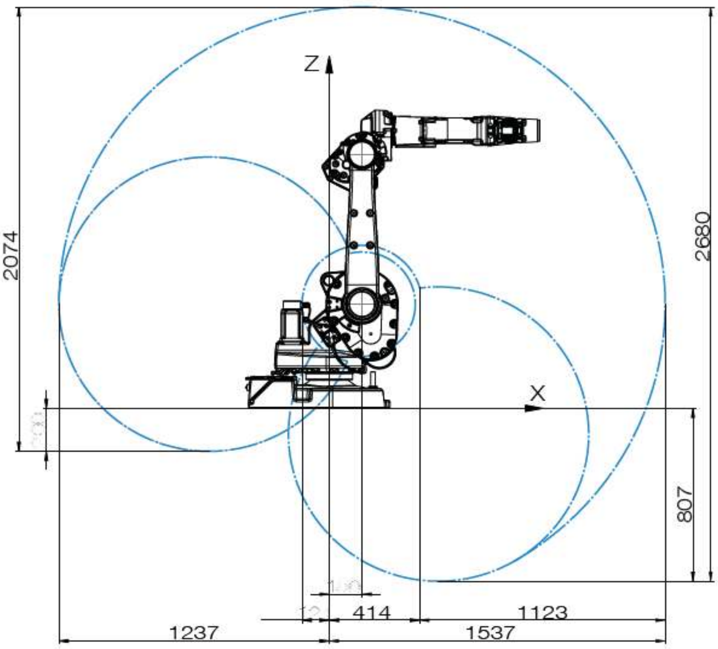

Figure 1.7 Industrial robot workspace illustration (ABB, 2016)

Especially, industrial robots are used in spot welding and arc welding applications (MIG/MAG, TIG and Plasma) whose method is performing continuous arc welding and these methods are performed well.

Advantages of robotic arc welding to conventional methods;

- High productivity
- Increased work safety
- High quality and strengthened weld seams

1.3.1 Robotic Welding Equipments

- Welding gun
- Wire feeder
- Power supplier
- Control unit
- Process gas
- Positioner

1.3.1.1 Positioners

Workpiece positioners have two main functions to contribute to robotic welding applications;

- Gaining additional degrees of freedom in manipulator/positioner configuration
- Performing more flexible simultaneous motion of robot and operator

While performing a welding task, robots have linear velocity between 0.75 m/sec and 1.5 m/sec. Actually, welding processs does not require to have more speed than 5 m/min because of robot’s displacement, robots are desired to move quickly if need.

Many of the welding robots have ±0.2 mm repeatability. These parameters are ±0.4 mm for MIG/MAG welding applications, ±0.1 mm for TIG welding applications. Also, maximum payloads of the robots which are generally used in arc welding applications are between 3-6 kg (Kaluç & Taban, 2004).

Today, there are many types of positioners designed to perform to move the welding workpiece. Some special welding positioners are illustrated below;

Figure 1.8 Two axis welding positioner (ABB, 2016)

Figure 1.9 Three axis welding positioner (IRCO Automation, 2016)

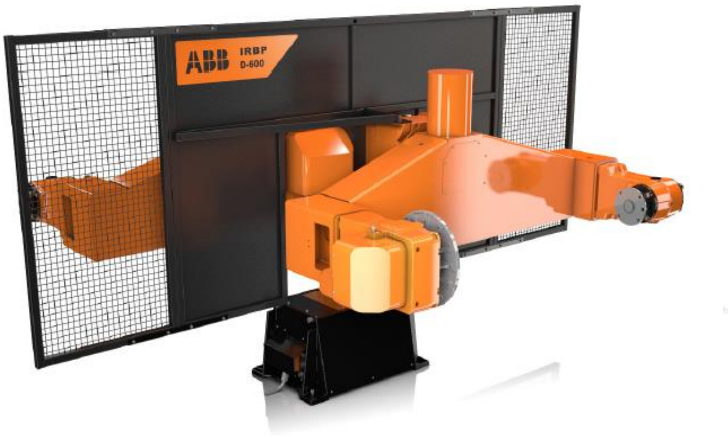

Figure 1.10 Four axis welding positioner (ABB, 2016)

CHAPTER TWO
PHYSICAL AND TOPOLOGICAL STRUCTURE

Three axis welding positioner system is comprised of four coordinate systems in joint space. The system has three degrees of freedom and three rotational links. The first two links perform motions just like a two link serial manipulator and the last link rotates perpendicular to the second link and there is an exantric joint configuration at this point.

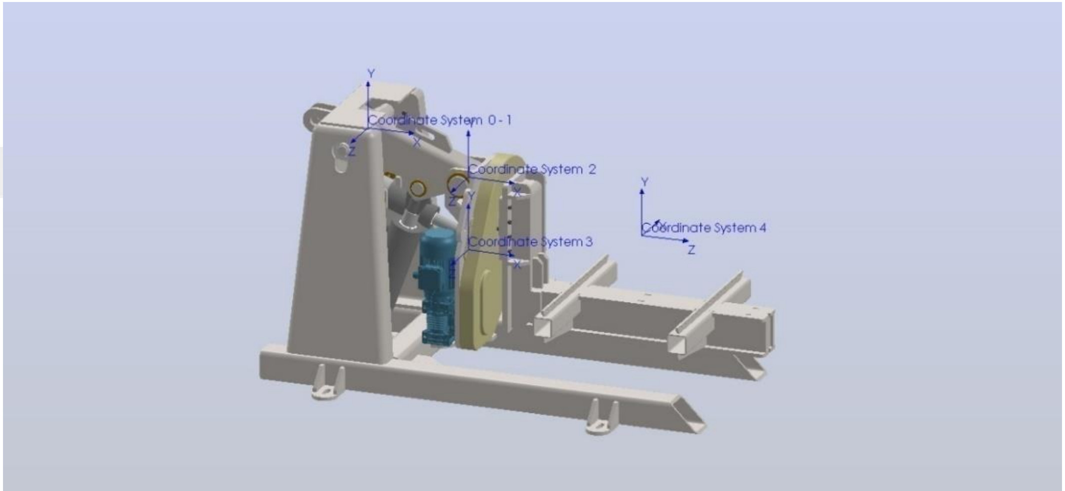

Figure 2.1 Welding positioner system

Figure 2.1 shows the actuators and the links. The first two links are actuated by hydraulic cylinders and the last link is actuated by electric motor. Hence, the system comprised of both hydraulic and electrical actuators, the system can be called hybrid manipulator system.

When the position of the output table is parallel to the right plane of the system, which will move like two parallel arms and the second hydraulic actuator will increase or decrease the tilt angle if need. Figure 2.2 shows the right plane of the system.

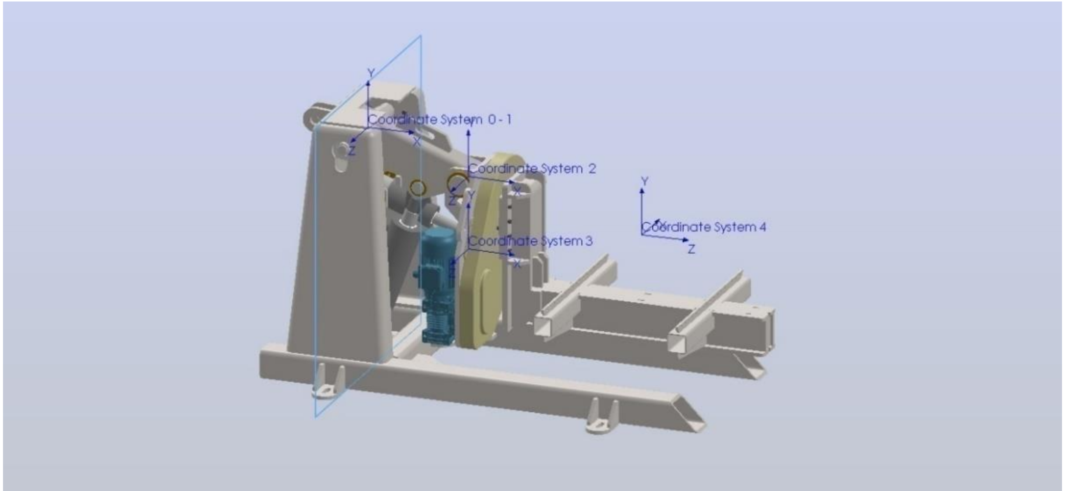

Figure 2.2 Right plane illustration

Kinematic structure is designed and shown in Figure 2.3. and Figure 2.4. Also members, joints, joint coordinate system positions and actuators are described in the system.

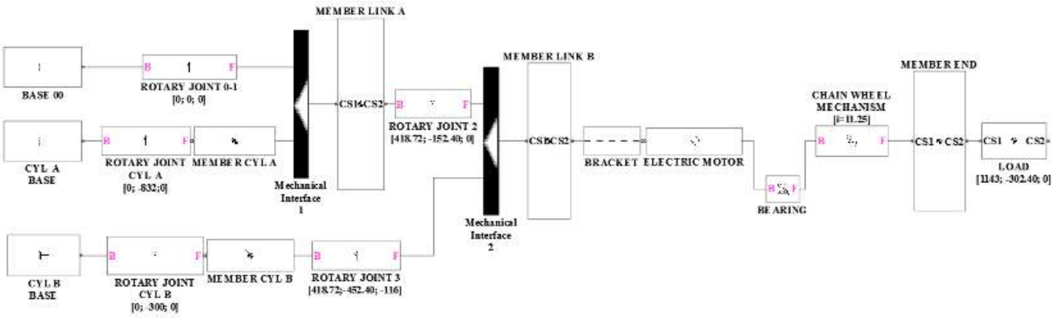

Figure 2.3 Kinematic structure

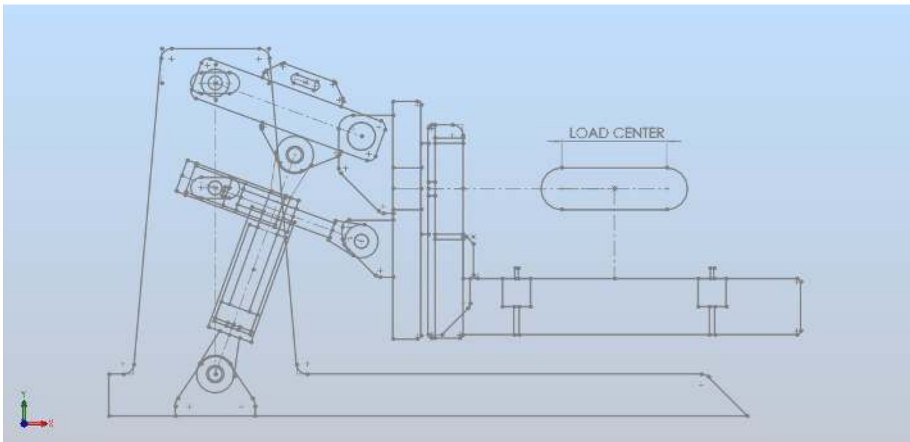

Figure 2.4 Sketch view

Also, Table 2.1 shows the joint space coordinate system positions respect to base coordinate system.

Table 2.1 Joint space coordinate system positions

Joint Coordinate System	Position $[P_x; P_y; P_z]$ [mm]
Coordinate System 0	[0; 0; 0]
Coordinate System 1	[0; 0; 0]
Coordinate System 2	[418.72; -152.40; 0]
Coordinate System 3	[418.72; -452.40; -116]
Coordinate System 4	[1143; -302.40; 0]

2.1 Actuators and Drive System

Tables which are shown below, describes the some basic spesifications of the actuators and drive system.

Table 2.2 Member cyl A

Member Cyl A	Diameter [mm]	Material	Stroke [mm]
Cylinder	$\emptyset 110 \times 130$	1.0050 (St 50-2)	234.91
Rod	$\emptyset 60$	1.0503 (C45)	

Table 2.3 Member Cyl B

Member Cyl B	Diameter [mm]	Material	Stroke [mm]
Cylinder	$\emptyset 80 \times 95$	1.0050 (St 50-2)	236.6
Rod	$\emptyset 45$	1.0503 (C45)	

Table 2.4 Electrical actuator

Electric Motor & Reductor	Power P_g [kW]	Output Rotation n_2 [rpm]	Output Torque M_2 [Nm]	Output Power P_2 [kW]	Reduction i
EV 075 2G80	0.37	9	185	0.17	100

Table 2.5 Chain drive system

Chain Mechanism	Teeth Number [Z]	Chain Type
Pinion	16	10B-1
Transmission Sprocket 1	32	10B-1
Transmission Sprocket 2	16	10B-1
Bull Gear	90	10B-1

2.2 Relative Motion Analysis

As seen from the system illustration, hydraulic cylinder one acts on to the first link which is called lifting arm and it rotates on the axis 1. And the second link rotates when the hydraulic cylinder two acts on it which is called rototable. The last link comprised of load beam and it is mounted on to the output plate of the rototable.

In the system the first link (lifting arm) moves as a parallel arm relative to the hydraulic cylinder two. This parallel arm mechanism has a translational motion with the electrical motor mounted rototable structure.

We see the axis 2 and axis 3 in Figure 2.1, there is a nonsliding rolling motion and the two point move together on the circular trajectories, because of this reason, the velocities become tangent to the trajectory. The system moves as a rigid body and there have been any relative motion between the each other. Hence, the velocities of these points are equal.

The second hydraulic cylinder acts on the second link (rototable) which moves and the tilt angle increases or decreases. Thus, the system is analysed with the relative motion with the rotary axis up to this part of the motion.

The formulation of Planar kinematics of rigid body and relative motion analysis are used for this problem;

$$V_B = V_A + \Omega x r_{B/A} + V_{B/A} \quad (2.1)$$

$$a_B = a_A + \dot{\Omega} x r_{B/A} + \Omega x (\Omega x r_{B/A}) + 2\Omega x V_{B/A} + a_{B/A} \quad (2.2)$$

2.3 Three Dimensional Motion Analysis

When the base coordinate system is chosen the axis 0; while the rotation center direction changes in the three dimensional space, the identified points with the axis generates a constant space cone.

In the system, the first two serial links and cylinders' relative rotary motion is described as precession motion and the rotary motion of the last link rototable is described as spin motion.

The resultant angular velocity;

$$w = w_P + w_S \tag{2.3}$$

2.4 Hydraulic Actuator Equations

2.4.1 Member Cyl A

Cosinus theorem is used for displacement equations of Member Cyl A. Also the computation is solved by using derivation for the equation.

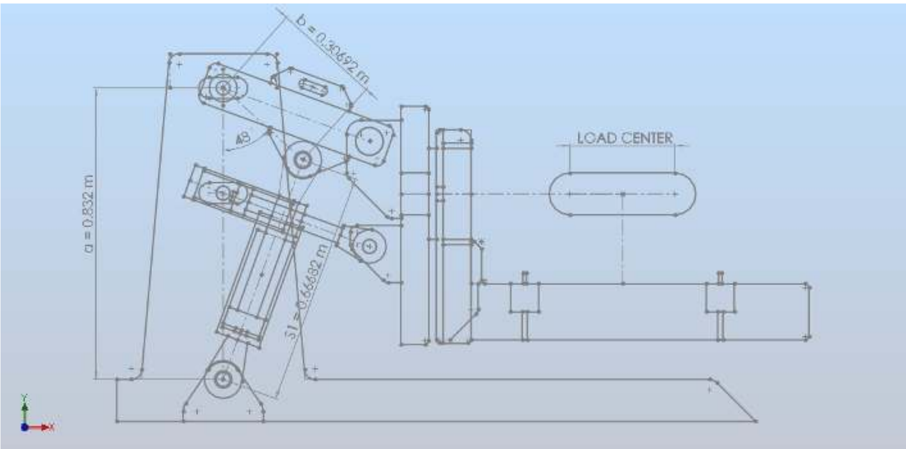

Figure 2.5 Dimensions of member cyl A

S_1; joint distance of Member Cyl A

a; distance between base coordinate and Member Cyl A joint

b; distance between base coordinate and Member Cyl A end joint

r_1; Member Cyl A displacement

θ_1; angular displacement of Member Link A

a= 0.832 [m]

b= 0.30692 [m]

$S_1 = 0.66682$ [m]

α=48°

$$S_1^{\ 2} = a^2 + b^2 - 2.a.b.\cos\alpha \qquad (2.4)$$

$$r_1 = 0.2846 \times \theta_1 \qquad (2.5)$$

2.4.2 Member Cyl B

Two different cosinus equations are used for displacement of Member Cyl B. Also the computation is solved by using derivation for the equations.

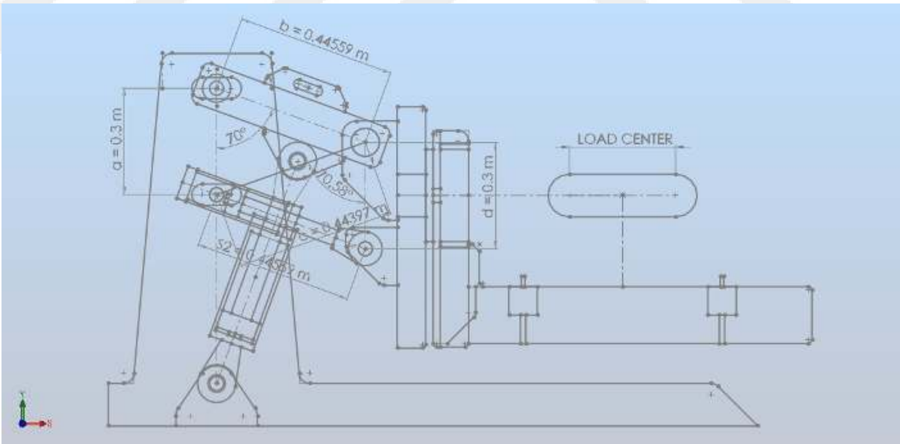

Figure 2.6 Dimensions of member cyl B

S_2; joint distance of Member Cyl B

r_2 ; Member Cyl B displacement

θ_2 ; angular displacement of Member Link B

a; distance between base coordinate system and joint of the Member Cyl B

b; joint distance of Member Link A

c; diagonal line

d; joint distance between coordinate system 2 and coordinate system 3

a= 0.3 [m]

b= 0.44559 [m]

c= 0.44397 [m]

d= 0.3 [m]

$S_2 = 0.44559$ [m]

φ= 70°

β=70.58°

2.4.2.1 Equation 1

$$c^2 = a^2 + b^2 - 2.a.b.\cos\varphi \tag{2.6}$$

2.4.2.2 Equation 2

$${S_2}^2 = c^2 + d^2 - 2.c.d.\cos\beta \tag{2.7}$$

$$r_2 = 0.282\theta_1 + 0.1795\dot{\theta}_1\theta_2 \tag{2.8}$$

CHAPTER THREE
MECHANICAL SYSTEM DESIGN

Mechanical system consists of eight main subassembly parts which are illustrated in Figure 3.1. Also, the system has three degrees of freedom and three rotational axis as it is mentioned before. As it is shown in the figure, the first two link is actuated by the hydraulic cylinders; Member Cyl A and Member Cyl B; the last link is actuated by an electric motor which triggers the output table and load beam by a chain wheel system. The mechanical system is mainly designed by welded steel sheet construction.

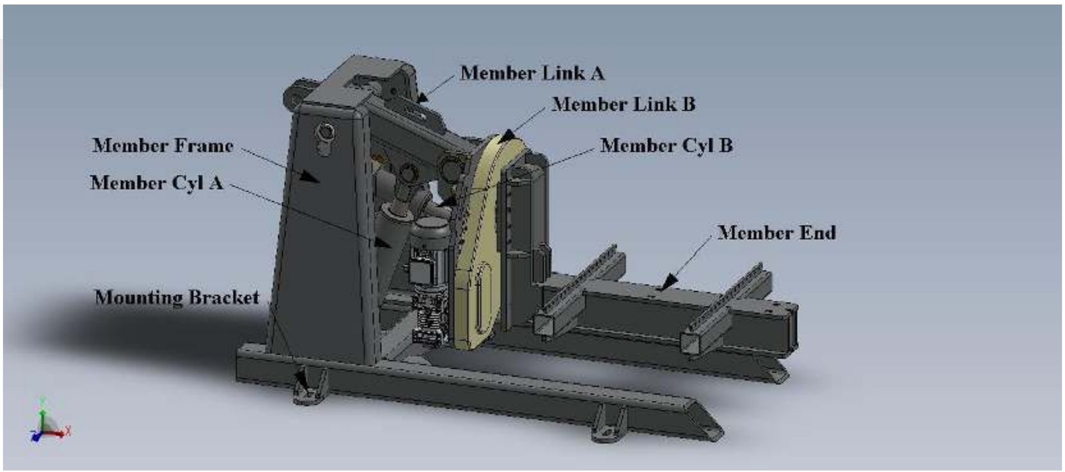

Figure 3.1 Mechanical system design

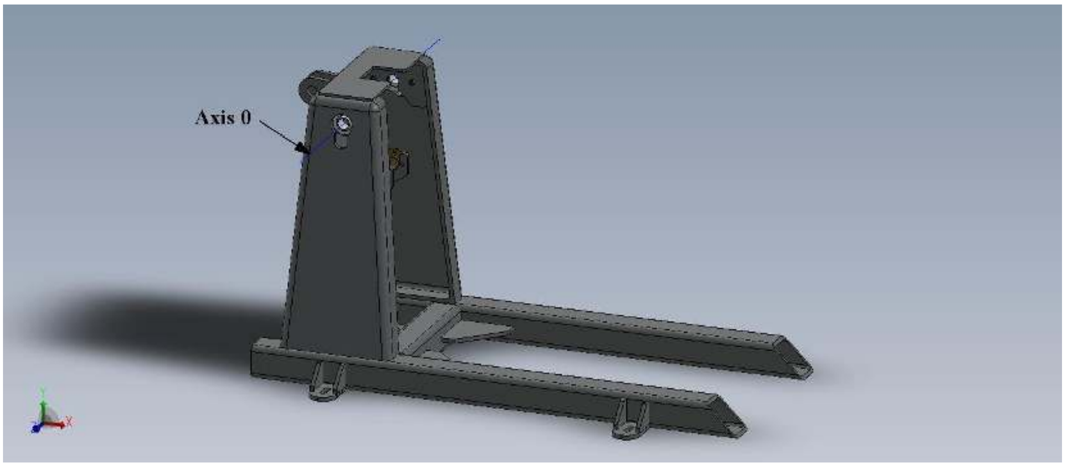

Figure 3.2 Member frame

Member frame consists of main body, carrier profiles, mounting brackets, bearing units and hydraulic cylinder mounting joint. Figure 3.2 shows Member frame.

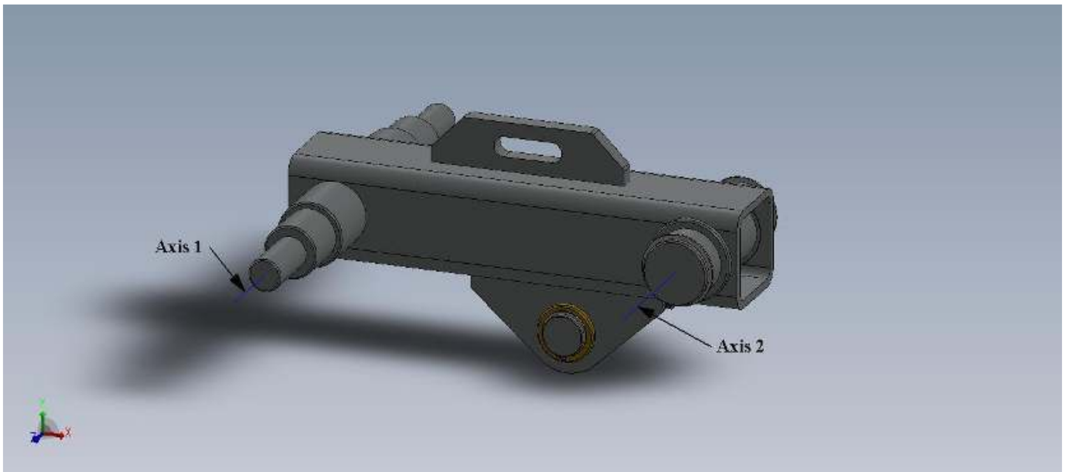

Figure 3.3 Member link A

Main parts of Member link A are carrier profile, grasping bracket, rotary joints and joint shafts. Figure 3.3 shows Member link A.

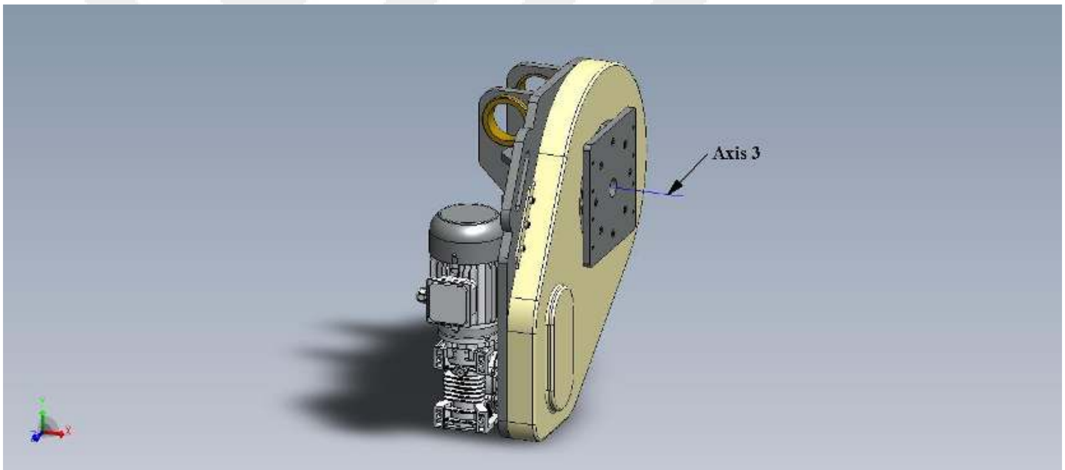

Figure 3.4 Member link B

Member Link B has more complex subassemblies than the other parts of the main system. The system consists of a mounting back plate which is constructed by a steel sheet and joint mounting brackets welded on its backside via the welding gaps. Also, there are main chain bullgear, pinion and chain mechanism on the front side of the back plate. The system is covered by a PE plastic cap via the mounting bolts. Finally, the system is mounted on to the output plate via the neck mounting sheet. Figure 3.4 shows Member link B.

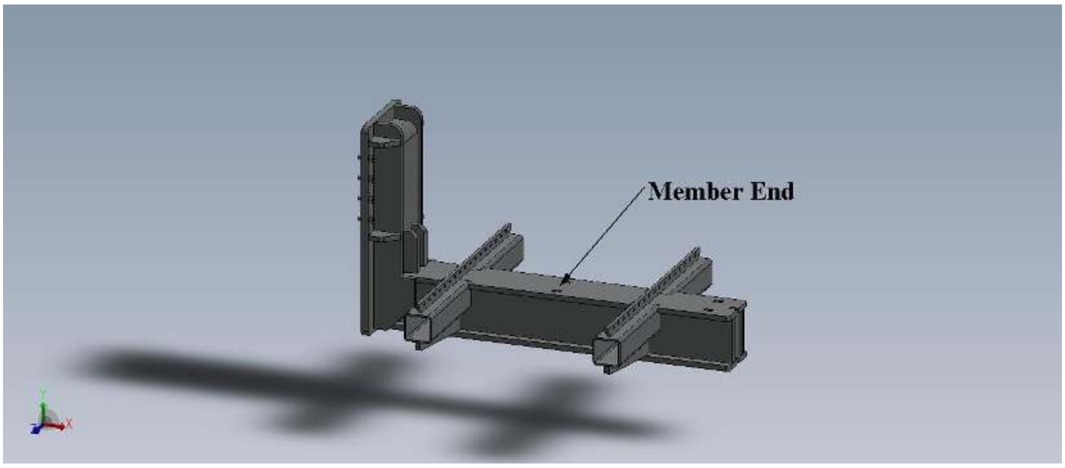

Figure 3.5 Member end

Member End consists of mounting backplate mounted on to the output plate, carrier profile sheets and carrier profiles, workpiece mounting flanges and mounting bolts. Main body is designed as a welded steel sheet construction. Figure 3.5 shows Member end.

The mechanical system has modular design concept criteria and main groups are designed welded steel sheet and bolted connection. In order to simplify the welding operations while manifacturing the system, welding gaps are designed on the sheets for simple welding operations.

Also the design is ergonomically thought and as considering the manifacturing and mounting operations; grasping gaps are designed for simple and quick plug and bolt holes for adjusting the member end and workpiece position orientation relative to the workpiece center of gravity.

CHAPTER FOUR
FINITE ELEMENT ANALYSIS SIMULATION

A simplified model is designed in the CAD tool for finite element analysis simulation. Also, as the contact areas, contact types and loading conditions are determined; stresses, strains and displacements are calculated at spesific positions in the FEA simulation program and finally results are obtained.

As a result of this simulation, revision design levels are handled and critical stress points and thicknesses are determined.

FEA positions are determined for five different loading conditions and member end loading condition for 1500 kg loading capacity and the results are calculated. Maximum Von Misses Theory is used for mathematical model for static structural stress analysis.

While starting the finite element analysis, load center positions are shown for every loading condition. Also, Figure 4.1 shows the simplified FEA model and Table 4.1 shows the load center positions.

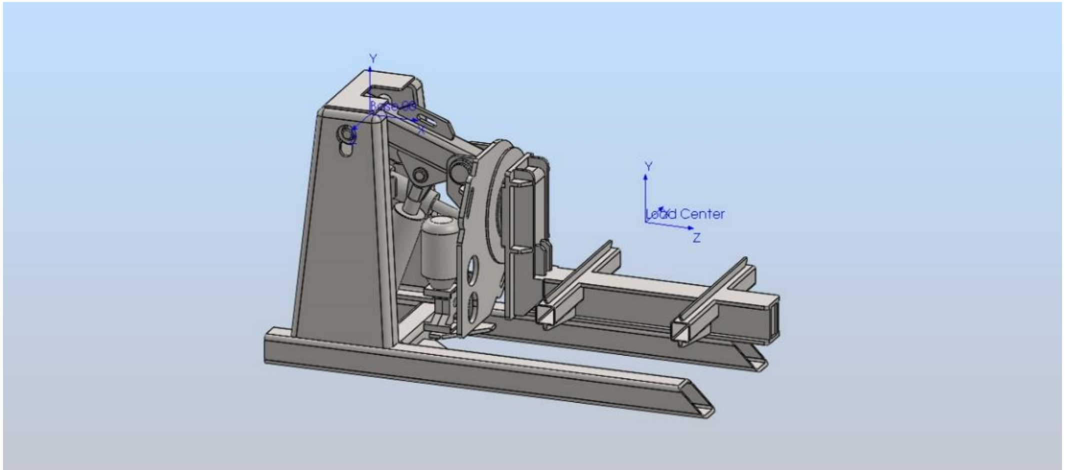

Figure 4.1 Simplified FEA model and load center

P_x is the distance of load center from the base coordinate system in x direction, P_y is the distance from the base coordinate system in y direction and θ_m is the motor angular displacement respect to the initial position.

Table 4.1 Load center positions

Analysis Position	Load Center Position [P_x; P_y; θ_m]
Analysis Position 1	[1143; -302.40; 0]
Analysis Position 2	[1169.87; -150; 0]
Analysis Position 3	[1128.12; 38.31; 0]
Analysis Position 4	[1138.53; 17.75; 0]
Analysis Position 5	[1123.65; 358.46; 0]

4.1 Structural Analysis

4.1.1 Analysis Position 1

- Maximum Von Misses stress emerging in the system at this position, is determined on the end point of the Member Cyl A and the resultant value is $\sigma_{max} = 173.41\ N/mm^2$. Also, the joint shaft material is chosen St 50-2 and maximum yield strength is $\sigma_y = 275\ N/mm^2$ and maximum tensile strength is $\sigma_t = 470\ N/mm^2$. $FoS = 1.5$ is obtained.

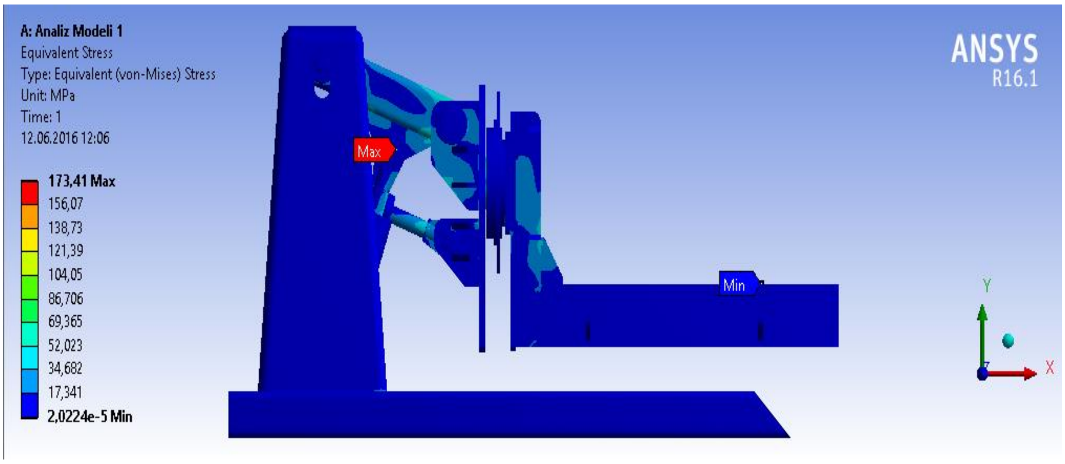

Figure 4.2 Analysis position 1 stress analysis result

- Maximum strain is determined on the joint mounting plate at the end point of the Member Cyl A.

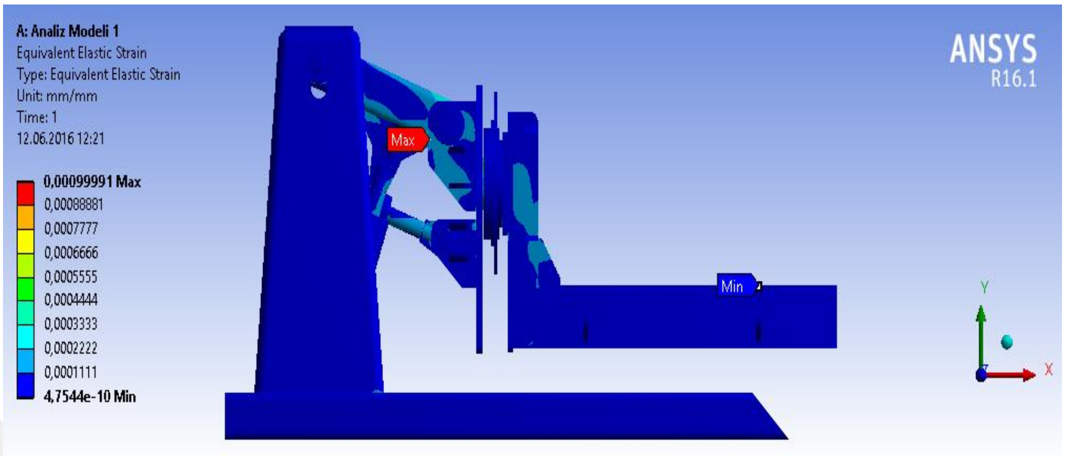

Figure 4.3 Analysis position 1 strain analysis result

- Mesh size parameter 10 mm is determined for the simulation analysis.

4.1.2 Analysis Position 2

- Maximum Von Misses stress emerging in the system is at the back end point of the Member Cyl A $\sigma_{max} = 215.38\ N/mm^2$ and $FoS = 1.3$ is obtained.

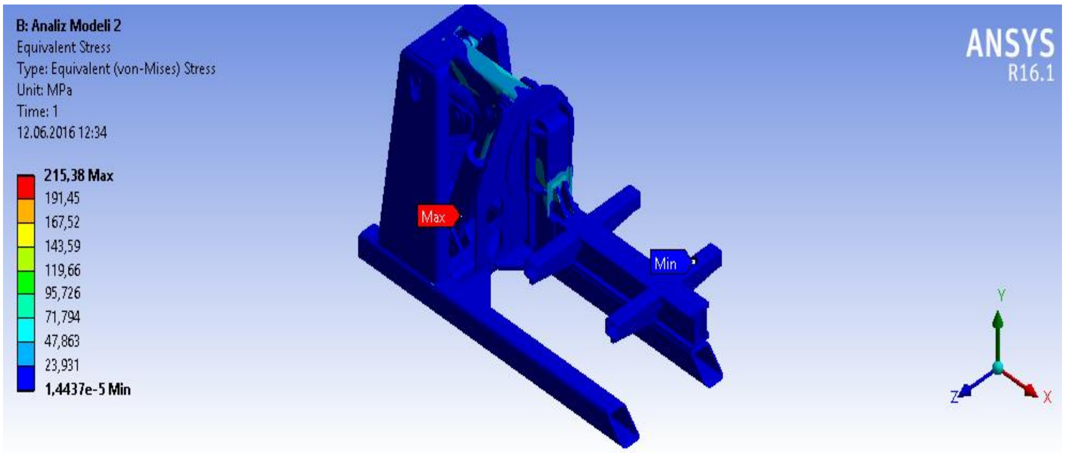

Figure 4.4 Analysis position 2 stress analysis result

- Maximum strain is determined on the joint mounting plate at the end point of the Member Cyl A.

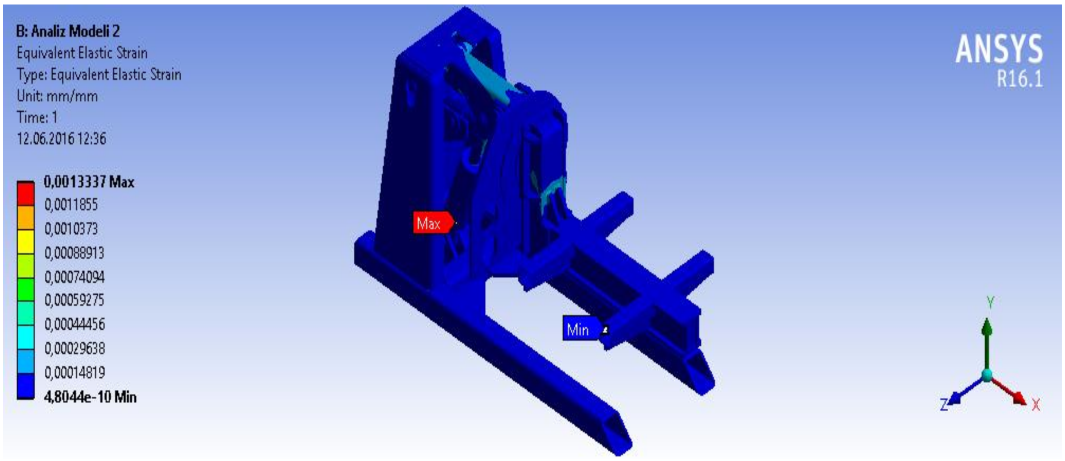

Figure 4.5 Analysis position 2 strain analysis result

- Mesh size parameter is determined 10 mm for the simulation analysis.

4.1.3 Analysis Position 3

- Maximum Von Misses emerging in the system is at the back joint of the Member Cyl A and the results are obtained as $\sigma_{max} = 225.71\ N/mm^2$ and $FoS = 1.2$ is obtained.

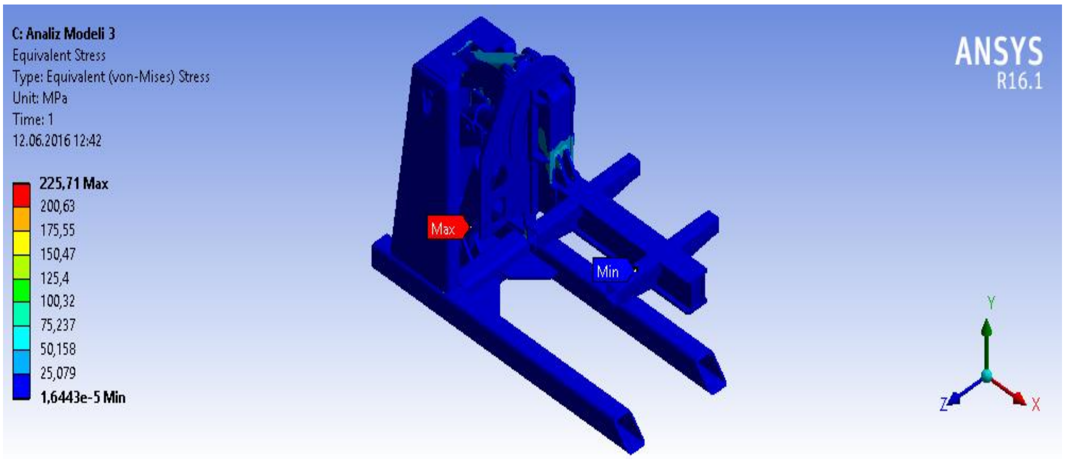

Figure 4.6 Analysis position 3 stress analysis result

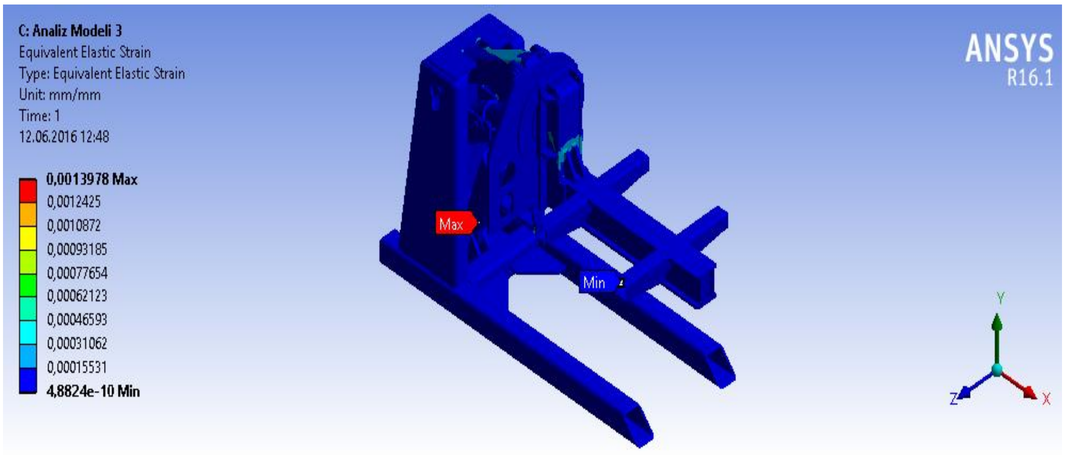

Figure 4.7 Analysis position 3 strain analysis result

- Mesh parameter size is determined 10 mm for the simulation analysis.

4.1.4 Analysis Position 4

- Maximum Von Misses stress emerging in the system is $\sigma_{max} = 178.48\ N/mm^2$ and $FoS = 1.5$ are obtained.

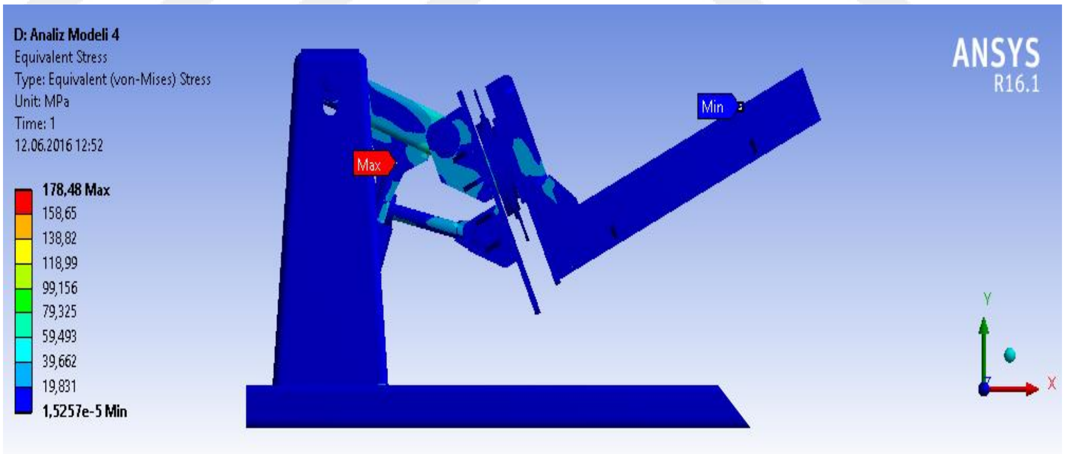

Figure 4.8 Analysis position 4 stress analysis result

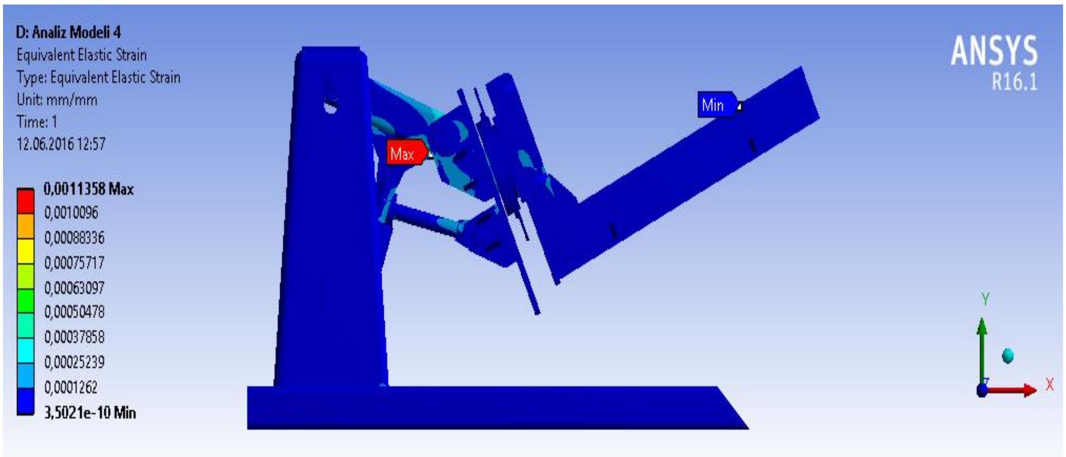

Figure 4.9 Analysis position 4 strain analysis result

- Mesh parameter size is determined 10 mm for the simulation analysis.

4.1.5 Analysis Position 5

- Maximum Von Misses stress emerging in the system $\sigma_{max} = 225.99\ N/mm^2$ and $FoS = 1.2$ are obtained.

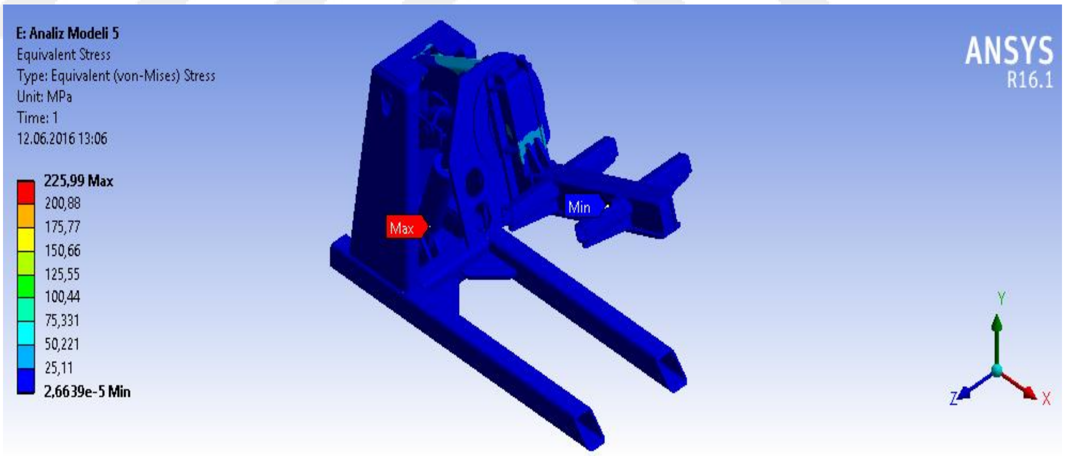

Figure 4.10 Analysis position 5 stress analysis result

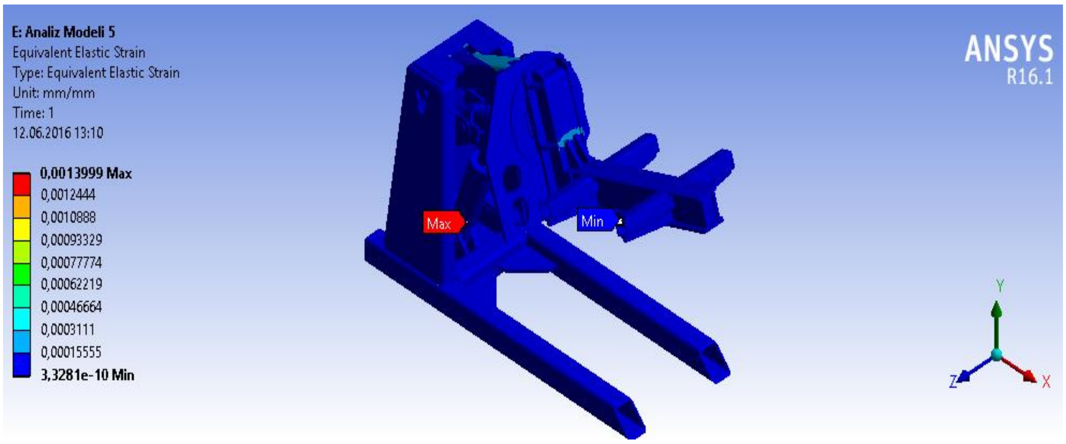

Figure 4.11 Analysis position 5 strain analysis result

- Mesh parameter size is determined 10 mm for the simulation analysis.

4.1.6 Member End Analysis

- Maximum Von Misses stress emerging $\sigma_{max} = 52.435\ N/mm^2$ and St 50-2 material is used for the construction of the assembly.
- $FoS = 5.5$ is obtained.

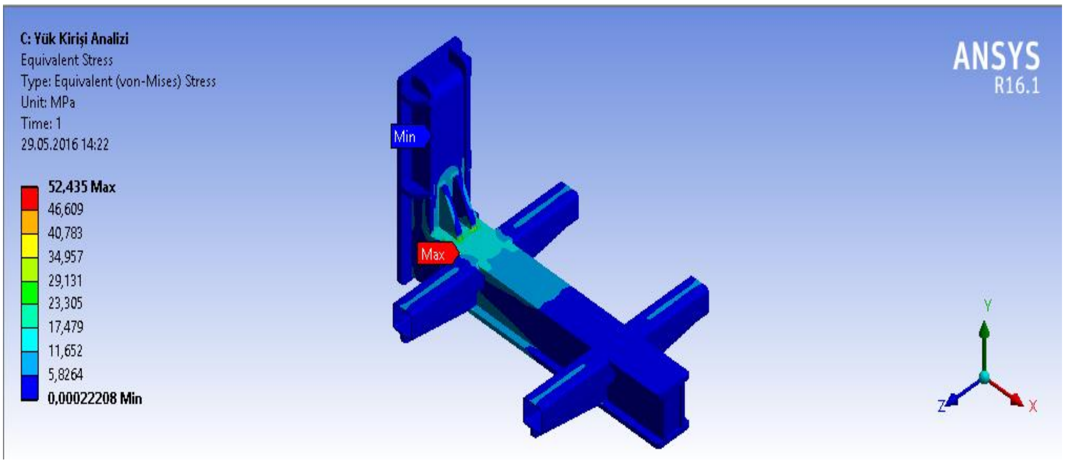

Figure 4.12 Member end stress analysis result

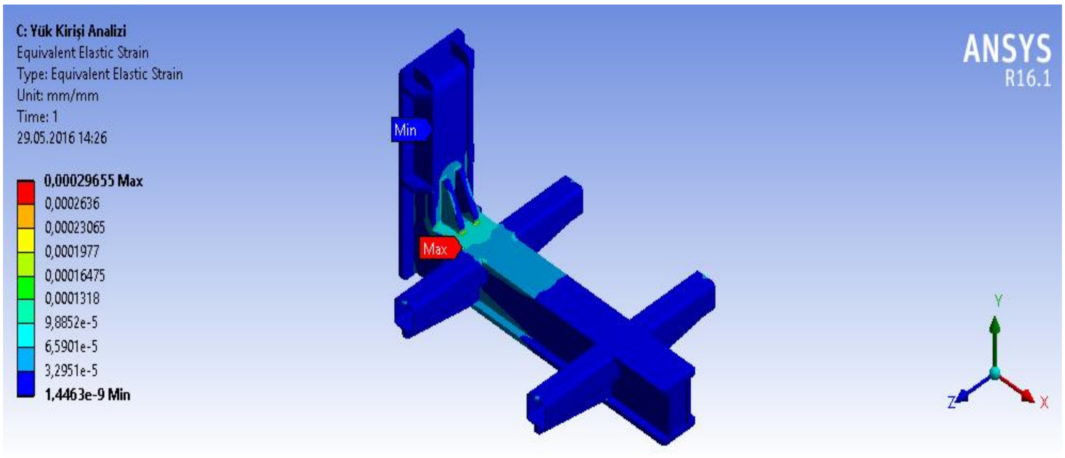

Figure 4.13 Member end strain analysis result

- Maximum elastic deformation emerging on the system is calculated at the end point of the member end and the resultant value 0.36 mm is obtained. But as a design criteria, displacement on the middle point of the structure is considered.

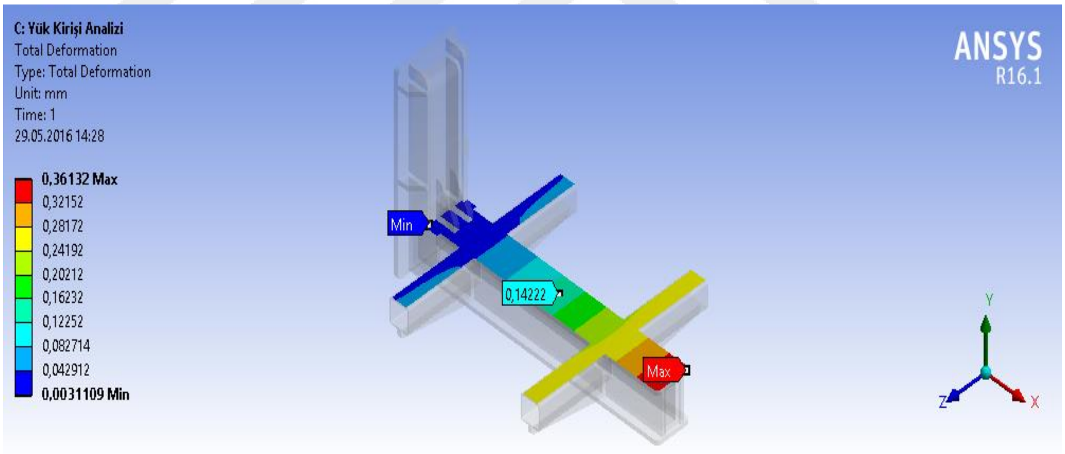

Figure 4.14 Member end displacement analysis result

4.2 Frequency Analysis

While starting the frequency analyses of five performance studies, initial and final positions are determined and used for the analyses. P_x is the distance from the base coordinate system in x direction, P_y is the distance from the base coordinate system in y direction and θ_m is the motor angular displacement respect to the initial position of the load center. Table 4.2 shows the initial and final positions of the end point.

Table 4.2 Frequency analysis positions

Task	Position [P_x; P_y; θ_m]
Initial Position	[1143; -302.40; 0]
Weld Path 1	[1157.14; -109.83; 0]
Weld Path 2	[1143; -302.40; 506.25°]
Weld Path 3	[1106.37; -332.35; 0]
Weld Path 4	[1033.14; -200.36; 0]
Weld Path 5	[1165.40; 170.15; 506.25°]

4.2.1 Weld Path 1

Table 4.3 shows the resonance frequencies and the figures show the frequency response graph and frequency modes of the analysis.

Table 4.3 Resonance frequencies

Mod No	Frequency [Rad/s]	Frequency [Hz]	Period [sec]
1	68.819	10.953	0.091301
2	94.342	15.015	0.0666
3	201.22	32.025	0.031226
4	207.39	33.007	0.030297
5	240.81	38.327	0.026091

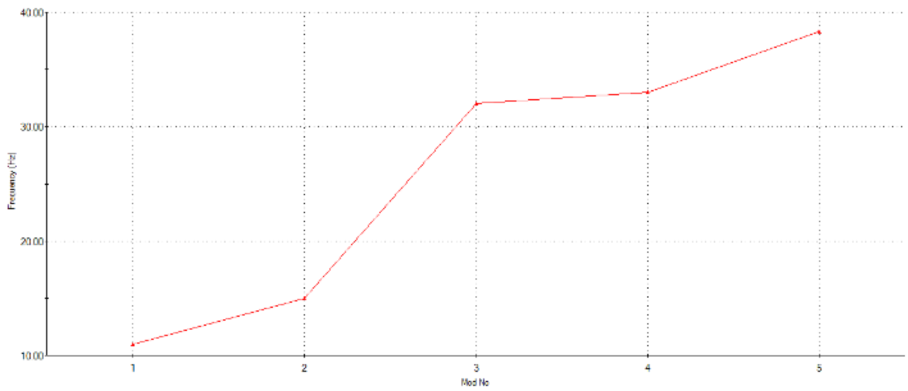

Figure 4.15 Frequency responses

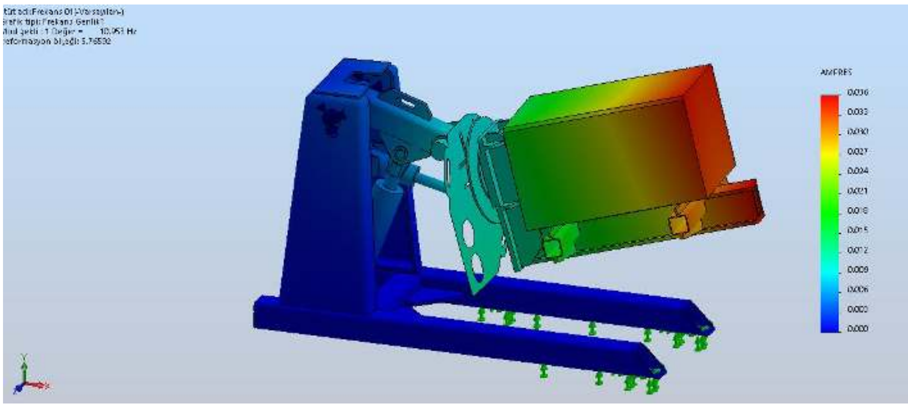

Figure 4.16 Frequency mod 1

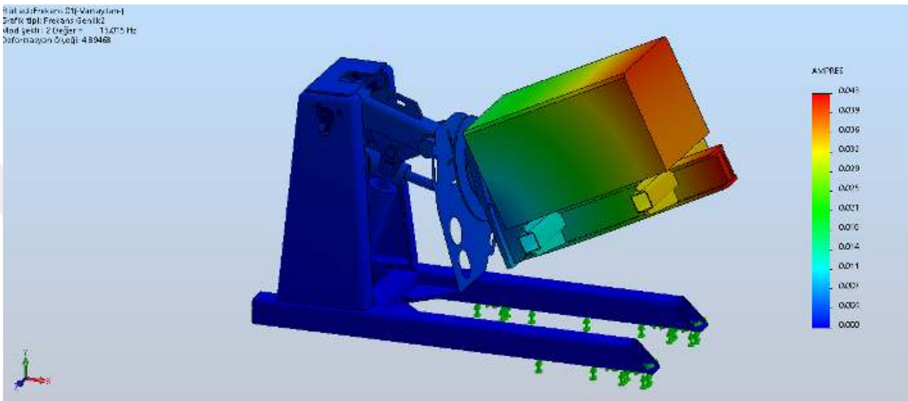

Figure 4.17 Frequency mod 2

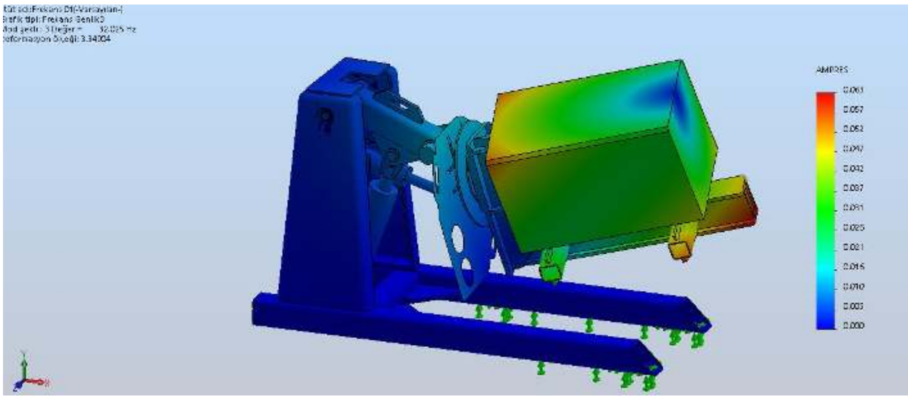

Figure 4.18 Frequency mod 3

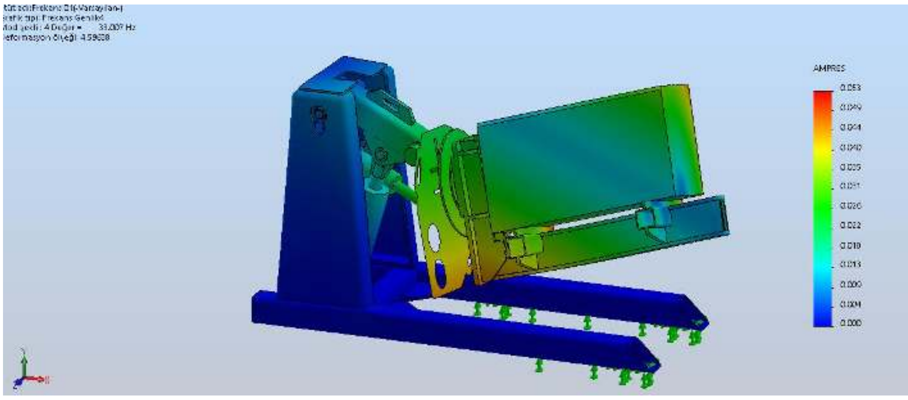

Figure 4.19 Frequency mod 4

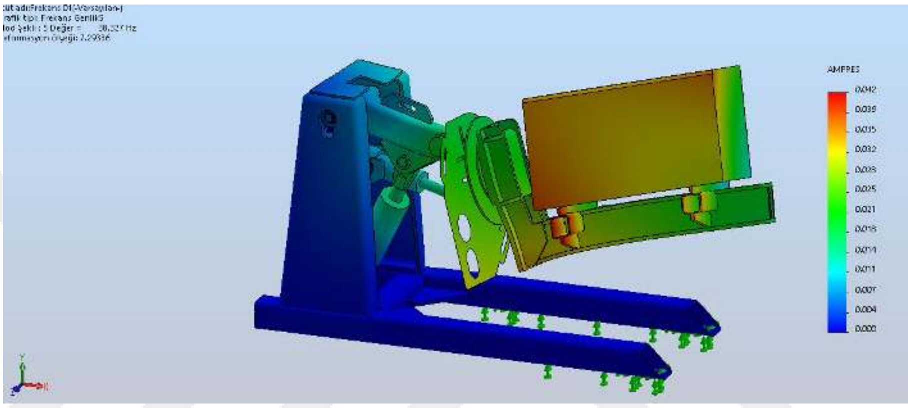

Figure 4.20 Frequency mod 5

4.2.2 Weld Path 2

Table 4.4 shows the resonance frequencies and the figures show the frequency response graph and frequency modes of the analysis.

Table 4.4 Resonance frequencies

Mod No	Frequency [Rad/s]	Frequency [Hz]	Period [sec]
1	70.671	11.248	0.088907
2	88.335	14.059	0.071129
3	199.15	31.695	0.03155
4	206.64	32.888	0.030406
5	251.93	40.096	0.02494

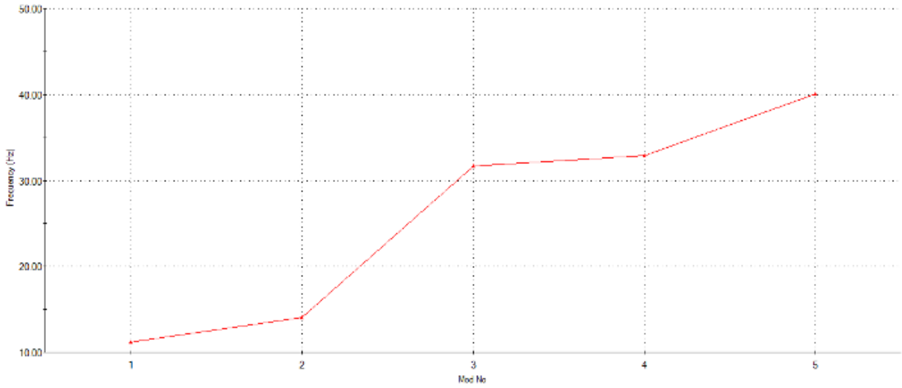

Figure 4.21 Frequency responses

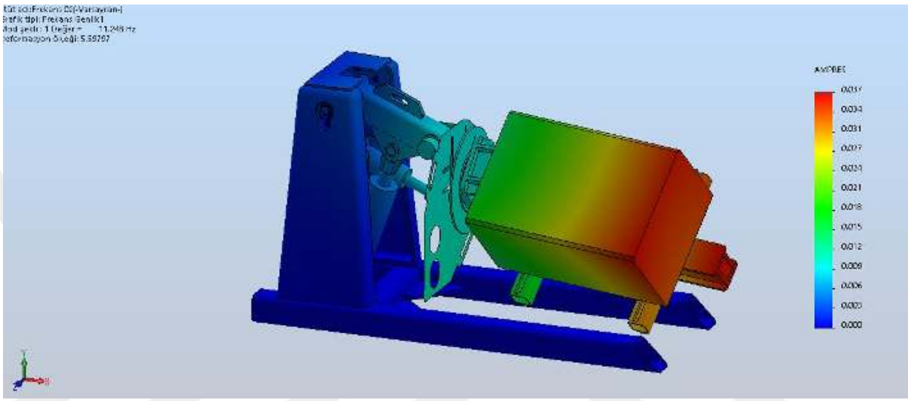
Figure 4.22 Frequency mod 1

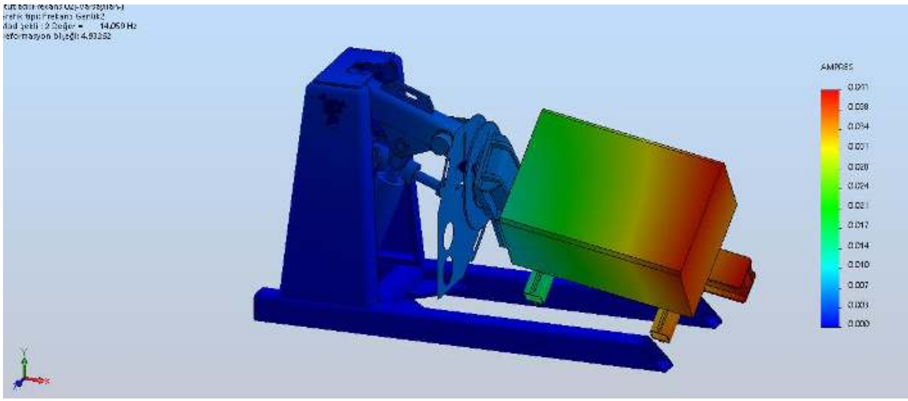
Figure 4.23 Frequency mod 2

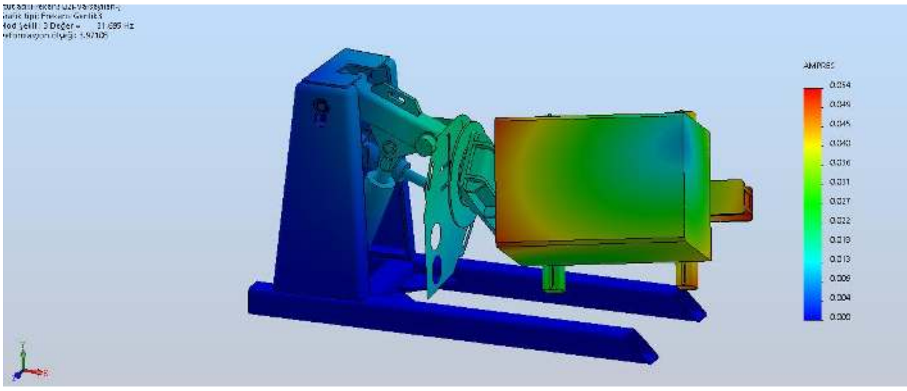

Figure 4.24 Frequency mod 3

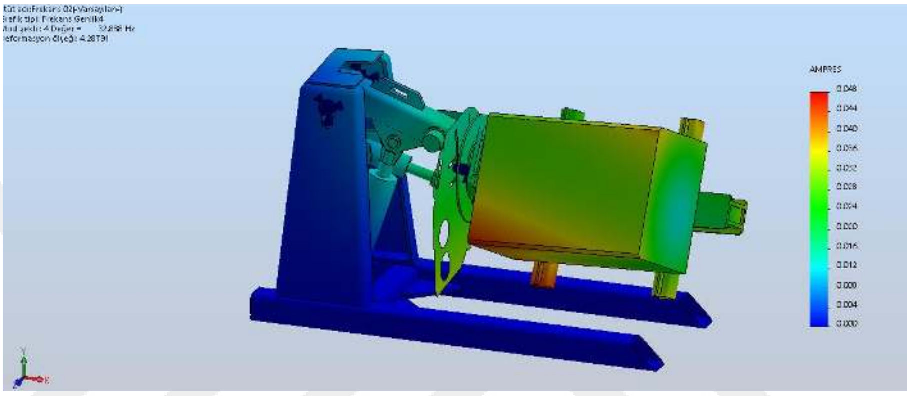

Figure 4.25 Frequency mod 4

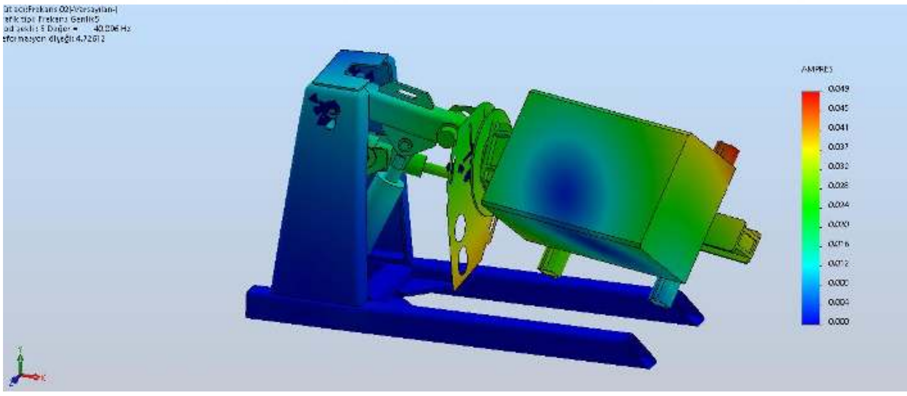

Figure 4.26 Frequency mod 5

4.2.3 Weld path 3

Table 4.5 shows the resonance frequencies and the figures show the frequency response graph and frequency modes of the analysis.

Table 4.5 Resonance frequencies

Mod No	Frequency [Rad/s]	Frequency [Hz]	Period [sec]
1	69.882	11.122	0.089912
2	93.781	14.926	0.066998
3	197.74	31.472	0.031775
4	217.52	34.62	0.028885
5	253.34	40.321	0.024801

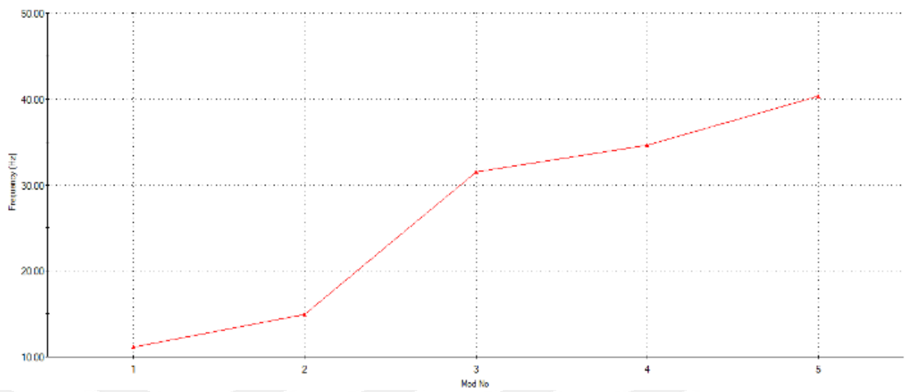

Figure 4.27 Frequency responses

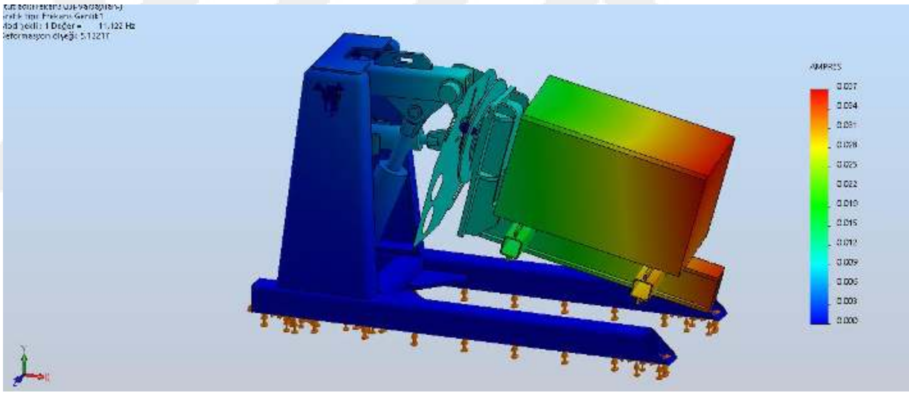

Figure 4.28 Frequency mod 1

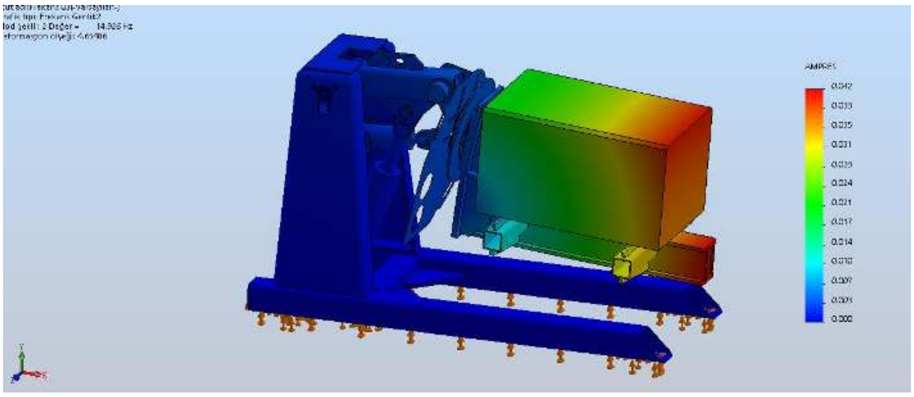

Figure 4.29 Frequency mod 2

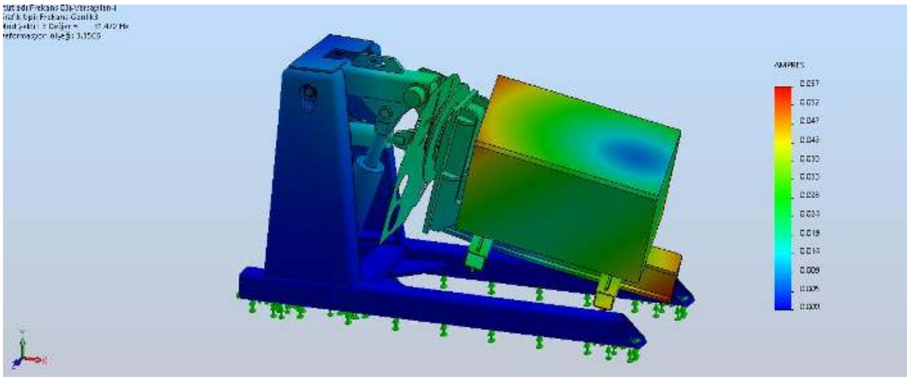

Figure 4.30 Frequency mod 3

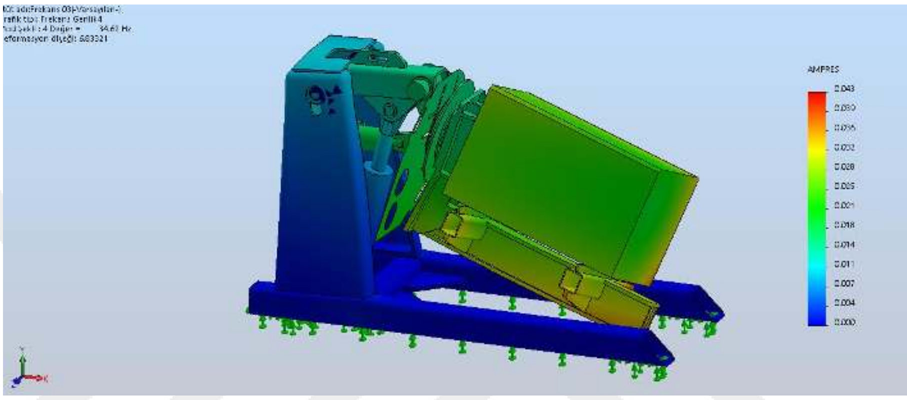

Figure 4.31 Frequency mod 4

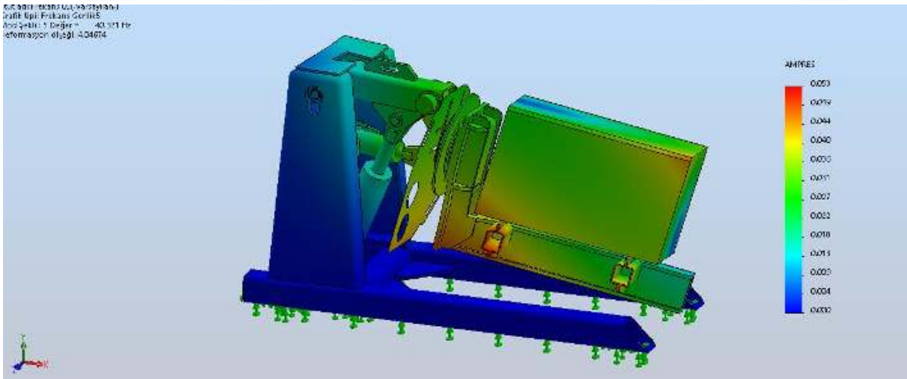

Figure 4.32 Frequency mod 5

4.2.4 Weld Path 4

Table 4.6 shows the resonance frequencies and the figures show the frequency response graph and frequency modes of the analysis.

Table 4.6 Resonance frequencies

Mod No	Frequency [Rad/s]	Frequency [Hz]	Period [sec]
1	70.779	11.265	0.088772
2	93.817	14.931	0.066973
3	179.01	28.491	0.035099
4	198.05	31.521	0.031725
5	248.99	39.629	0.025234

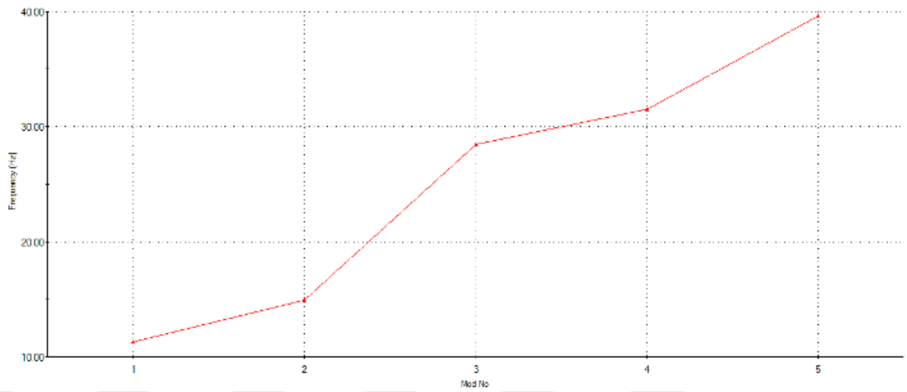

Figure 4.33 Frequency responses

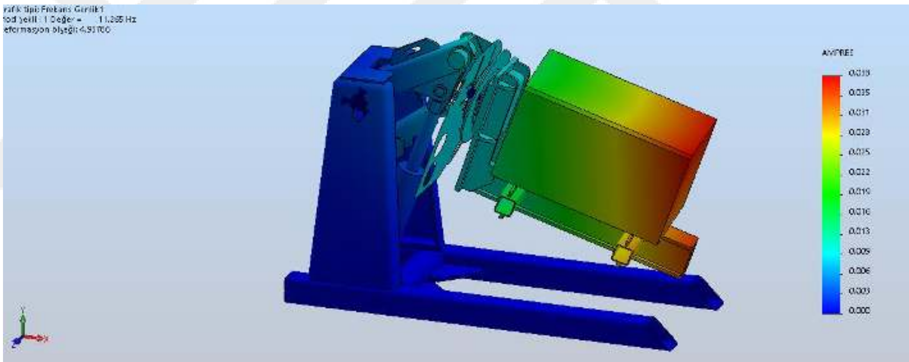

Figure 4.34 Frequency mod 1

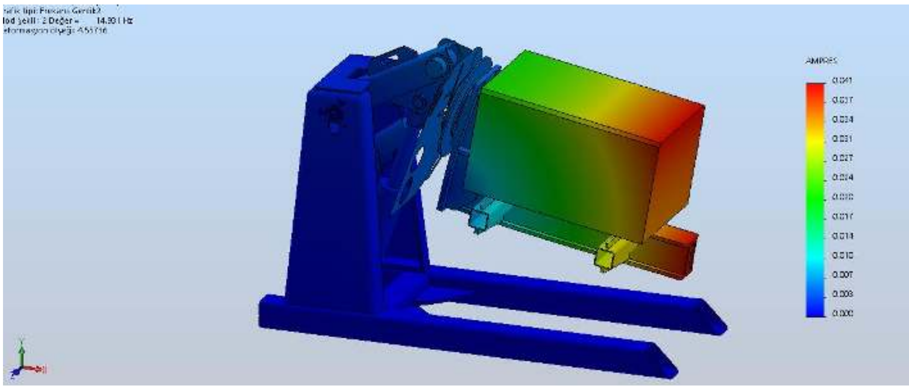

Figure 4.35 Frequency mod 2

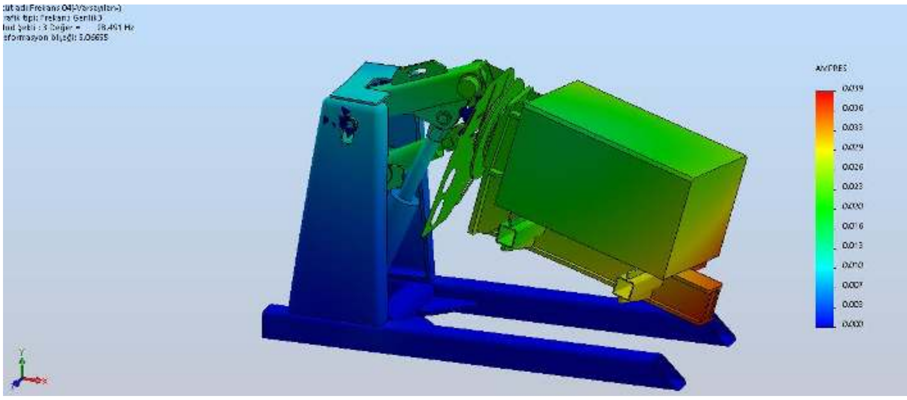

Figure 4.36 Frequency mod 3

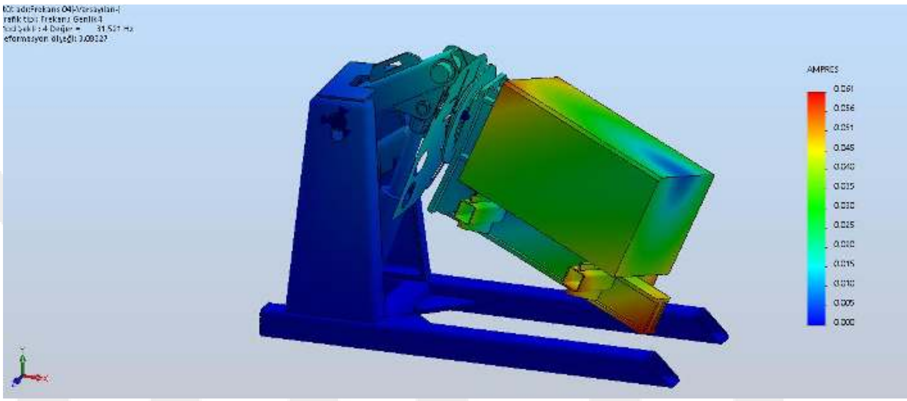

Figure 4.37 Frequency mod 4

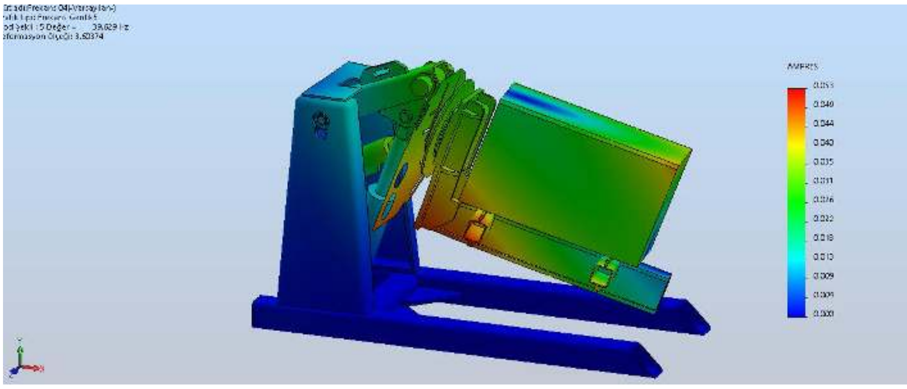

Figure 4.38 Frequency mod 5

4.2.5 Weld Path 5

Table 4.7 shows the resonance frequencies and the figures show the frequency response graph and frequency modes of the analysis.

Table 4.7 Resonance frequencies

Mod No	Frequency [Rad/s]	Frequency [Hz]	Period [sec]
1	69.639	11.083	0.090225
2	86.533	13.772	0.072611
3	201.18	32.019	0.031231
4	205.5	32.706	0.030575
5	271.61	43.228	0.023133

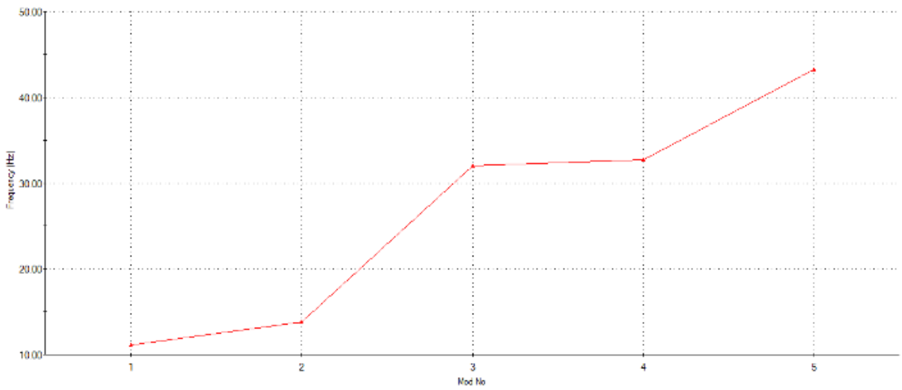

Figure 4.39 Frequency responses

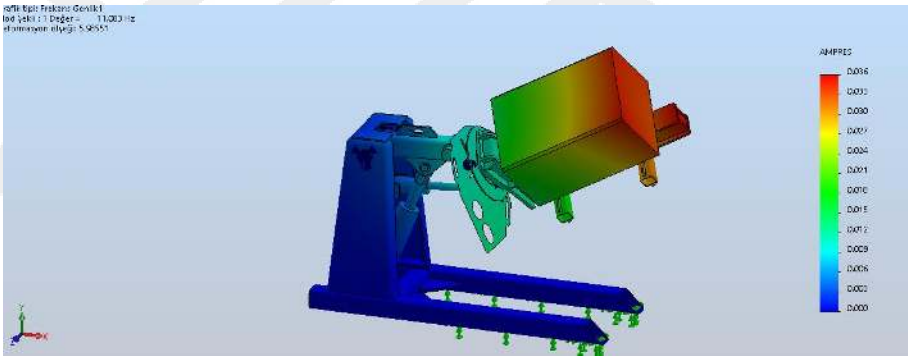
Figure 4.40 Frequency mod 1

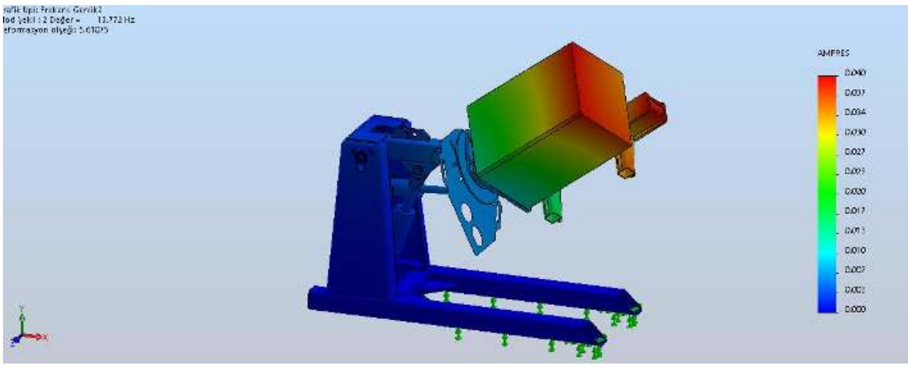
Figure 4.41 Frequency mod 2

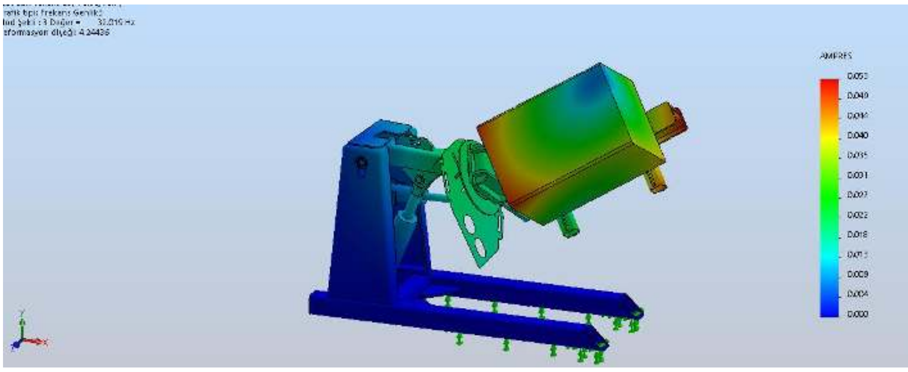

Figure 4.42 Frequency mod 3

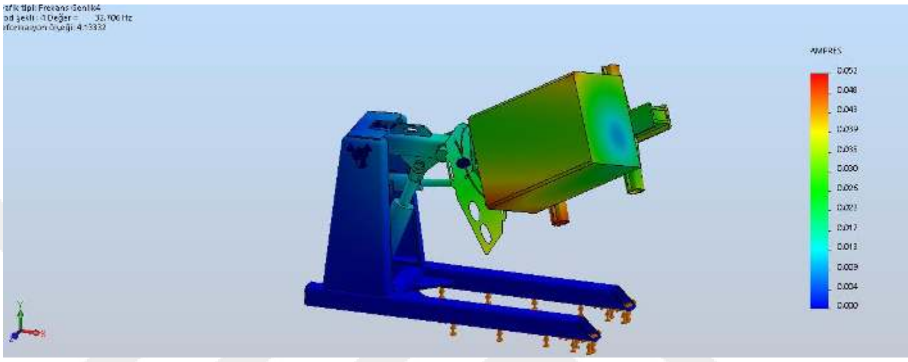

Figure 4.43 Frequency mod 4

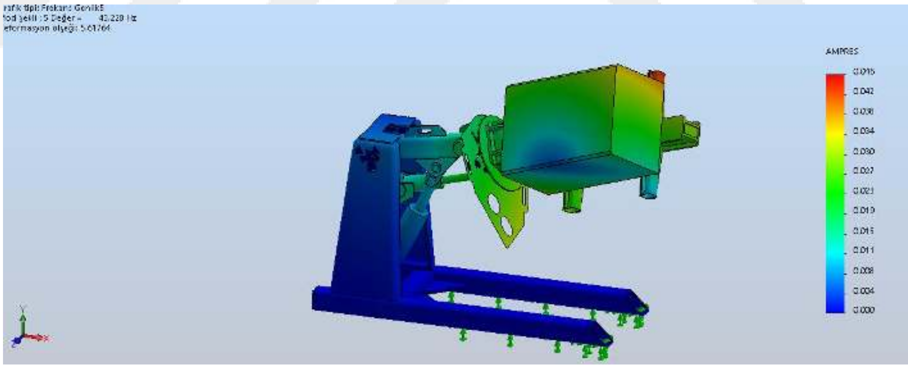

Figure 4.44 Frequency mod 5

CHAPTER FIVE
KINEMATIC ANALYSIS AND JACOBIAN

The position analysis of the system is solved by choosing a coordinate system for every single axis, Z axis is rotation direction and 0-1 coordinate system are coincident. Coordinate system 4 is the center of gravity of the workpiece and concentric with the rotation center of the member end. Figure 5.1 shows the coordinate systems.

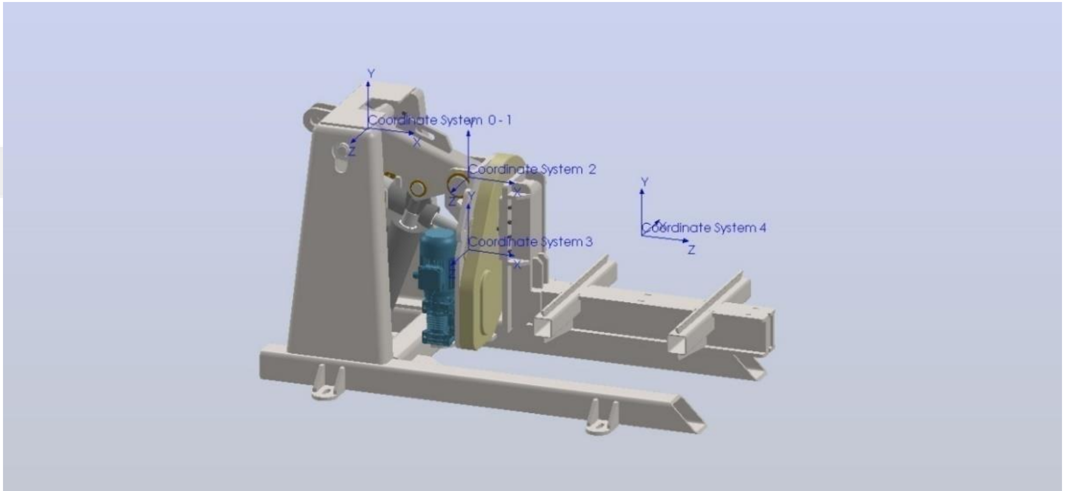

Figure 5.1 Coordinate system configuration

The system is starting its motion from the initial condition and the load center is on the coordinate system 4 and Table 5.1 shows the initial and final position of the end point.

Table 5.1 Load center positions

Condition	Load Center Position [P_x; P_y; θ_m]
Initial Position	[1143; -302.40; 0]
Final Position	[1165.40; 170.15; 1012.5°]

5.1 Kinematic Position Analysis

- The forward kinematic solution of the system is obtained by using homogen transformation matrice method;

$$ {}^{0}_{4}T = {}^{0}_{1}T\,{}^{1}_{2}T\,{}^{2}_{3}T\,{}^{3}_{4}T \tag{5.1} $$

- θ_1 rotation on the coordinate systems 0-1 is ${}^{0}_{1}R$ matrice;

$$ {}^{0}_{1}R = [{}^{0}X_1 \quad {}^{0}Y_1 \quad {}^{0}Z_1] = \begin{bmatrix} X_1X_0 & Y_1X_0 & Z_1X_0 \\ X_1Y_0 & Y_1Y_0 & Z_1Y_0 \\ X_1Z_0 & Y_1Z_0 & Z_1Z_0 \end{bmatrix} = \begin{bmatrix} \cos\theta_1 & -\sin\theta_1 & 0 \\ \sin\theta_1 & \cos\theta_1 & 0 \\ 0 & 0 & 1 \end{bmatrix} \tag{5.2} $$

- ${}^{0}_{1}T^{-1}$ the inverse homogen transformation matrce is;

$$ {}^{0}_{1}T^{-1} = \begin{bmatrix} {}^{0}_{1}R^{T} & -{}^{0}_{1}R^{T}\,{}^{0}_{1}P \\ 0\ 0\ 0 & 1 \end{bmatrix} \tag{5.3} $$

$$ {}^{0}_{1}R^{T} = \begin{bmatrix} \cos\theta_1 & \sin\theta_1 & 0 \\ -\sin\theta_1 & \cos\theta_1 & 0 \\ 0 & 0 & 1 \end{bmatrix} \tag{5.4} $$

$$ {}^{0}_{1}R^{T}\,{}^{0}_{1}P = \begin{bmatrix} \cos\theta_1 & \sin\theta_1 & 0 \\ -\sin\theta_1 & \cos\theta_1 & 0 \\ 0 & 0 & 1 \end{bmatrix} \begin{bmatrix} 0 \\ 0 \\ 0 \end{bmatrix} \tag{5.5} $$

$$ {}^{0}_{1}T^{-1} = \begin{bmatrix} \cos\theta_1 & \sin\theta_1 & 0 & 0 \\ -\sin\theta_1 & \cos\theta_1 & 0 & 0 \\ 0 & 0 & 1 & 0 \\ 0 & 0 & 0 & 1 \end{bmatrix} \tag{5.6} $$

- θ_2 rotation on the coordinate systems 1-2 ${}^{1}_{2}R$ matrice is;

$$ {}^{1}_{2}R = [{}^{1}X_2 \quad {}^{1}Y_2 \quad {}^{1}Z_2] = \begin{bmatrix} X_2X_1 & Y_2X_1 & Z_2X_1 \\ X_2Y_1 & Y_2Y_1 & Z_2Y_1 \\ X_2Z_1 & Y_2Z_1 & Z_2Z_1 \end{bmatrix} = \begin{bmatrix} \cos\theta_2 & -\sin\theta_2 & 0 \\ \sin\theta_2 & \cos\theta_2 & 0 \\ 0 & 0 & 1 \end{bmatrix} \tag{5.7} $$

- ${}^{1}_{2}T$ homogen transformation matrice is;

$$ {}^{1}_{2}T = \begin{bmatrix} \cos\theta_2 & -\sin\theta_2 & 0 & 418.72 \\ \sin\theta_2 & \cos\theta_2 & 0 & -152.40 \\ 0 & 0 & 1 & 0 \\ 0 & 0 & 0 & 1 \end{bmatrix} \tag{5.8} $$

- Coordinate systems 2-3 ${}^{2}_{3}R$ matrice is;

$$ {}^{2}_{3}R = [{}^{2}X_3 \quad {}^{2}Y_3 \quad {}^{2}Z_3] = \begin{bmatrix} X_3X_2 & Y_3X_2 & Z_3X_2 \\ X_3Y_2 & Y_3Y_2 & Z_3Y_2 \\ X_3Z_2 & Y_3Z_2 & Z_3Z_2 \end{bmatrix} = \begin{bmatrix} 1 & 0 & 0 \\ 0 & 1 & 0 \\ 0 & 0 & 1 \end{bmatrix} \tag{5.9} $$

- ${}^{2}_{3}T$ homogen transformation matrice is;

$$ {}^{2}_{3}T = \begin{bmatrix} 1 & 0 & 0 & 0 \\ 0 & 1 & 0 & -300 \\ 0 & 0 & 1 & 0 \\ 0 & 0 & 0 & 1 \end{bmatrix} \tag{5.10} $$

- θ_3 rotation on the coordinate systems 3-4 ${}^{3}_{4}R$ matrice is;

$$ {}^{3}_{4}R = [{}^{3}X_4 \quad {}^{3}Y_4 \quad {}^{3}Z_4] = \begin{bmatrix} X_4X_3 & Y_4X_3 & Z_4X_3 \\ X_4Y_3 & Y_4Y_3 & Z_4Y_3 \\ X_4Z_3 & Y_4Z_3 & Z_4Z_3 \end{bmatrix} = \begin{bmatrix} 0 & 0 & 1 \\ \sin\theta_3 & \cos\theta_3 & 0 \\ -\cos\theta_3 & \sin\theta_3 & 0 \end{bmatrix} \tag{5.11} $$

- ${}^{3}_{4}T$ homogen transformation matrice is;

$$ {}^{2}_{3}T = \begin{bmatrix} 0 & 0 & 1 & 724.28 \\ \sin\theta_3 & \cos\theta_3 & 0 & 150 \\ -\cos\theta_3 & \sin\theta_3 & 0 & 0 \\ 0 & 0 & 0 & 1 \end{bmatrix} \tag{5.12} $$

- Orientation matrice of the 0-4 coordinate systems is;

$$ {}^{0}_{4}R = [{}^{0}X_4 \quad {}^{0}Y_4 \quad {}^{0}Z_4] = \begin{bmatrix} X_4X_0 & Y_4X_0 & Z_4X_0 \\ X_4Y_0 & Y_4Y_0 & Z_4Y_0 \\ X_4Z_0 & Y_4Z_0 & Z_4Z_0 \end{bmatrix} \tag{5.13} $$

- ${}^{0}_{4}T$ homogen transformation matrice is;

$$ {}^{0}_{4}T = \begin{bmatrix} -0.4226 & 0 & 0.9063 & 1165.40 \\ 0.9063 & 0 & 0.4226 & 170.15 \\ 0 & 1 & 0 & 0 \\ 0 & 0 & 0 & 1 \end{bmatrix} \tag{5.14} $$

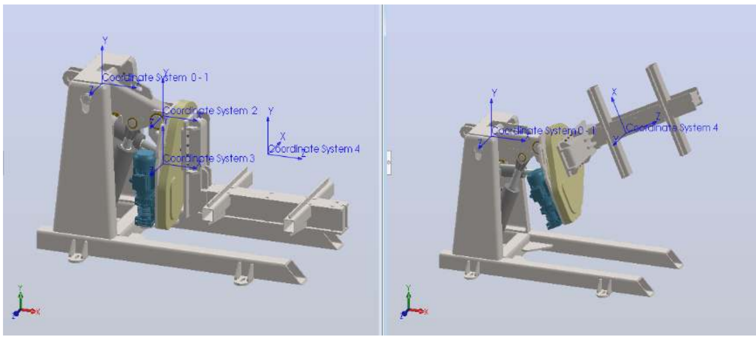

Figure 5.2 System position illustration

- Inverse kinematic solution of the system is;

$$ {}^{0}_{1}[T]^{-1}\,{}^{0}_{4}T = {}^{1}_{2}T\,{}^{2}_{3}T\,{}^{3}_{4}T \qquad (5.15) $$

- Resultant equations of the matrice multiplications;

$r_{11} = 0.9063 \sin\theta_1 - 0.4226 \cos\theta_1 = -\sin\theta_2 \sin\theta_3$

$r_{13} = 0.4226 \sin\theta_1 - 0.9063 \cos\theta_1 = \cos\theta_2$

$r_{14} = 170.15 \sin\theta_1 + 1165.40 \cos\theta_1 = 150 \sin\theta_2 + 724.28 \cos\theta_2 + 418.72$

$r_{21} = 0.4226 \sin\theta_1 - 0.9063 \cos\theta_1 = \cos\theta_2 \sin\theta_3$

$r_{23} = -0.9063 \sin\theta_1 + 0.4226 \cos\theta_1 = \sin\theta_2$

$r_{24} = -1165.40 \sin\theta_1 + 170.15 \cos\theta_1 = 724.28 \sin\theta_2 - 150 \cos\theta_2 - 152.40$

$r_{31} = -\cos\theta_3$

$r_{32} = \sin\theta_3 = 1 \quad \rightarrow \arcsin 1 = \theta_3 = 90°$

$r_{13} - r_{14} - r_{23}$ equations;

$170.15 \sin\theta_1 + 1165.40 \cos\theta_1 = 150[-0.9063 \sin\theta_1 + 0.4226 \cos\theta_1] +$

$724.28[0.4226 \sin\theta_1 - 0.9063 \cos\theta_1] + 418.72$

$0.014272 \sin\theta_1 + 445.595036 \cos\theta_1 = 418.72$

$\theta_1 = \text{Atan2}(0.014272; 445.595036) \pm$

$\text{Atan2}(\sqrt{0.014272^2 + 445.595036^2 - 418.72^2}; 418.72)$

$$ \theta_1 = 20° \quad \theta_2 = 5° \qquad (5.16) $$

5.2 Jacobian

The velocity of the coordinate system 4 with respect to the base coordinate system 0 is solved by the iterative calculation method.

- For i=0 angular velocity;

$$ {}^{0}w_0 = [0 \quad 0 \quad 0]^{T} \tag{5.17}$$

$$ {}^{1}_{0}R = {}^{0}_{1}R^{T} \tag{5.18}$$

$$ {}^{1}w_1 = {}^{1}_{0}R\,{}^{0}w_0 + \dot{\theta}_1\,{}^{1}Z_1 \tag{5.19}$$

$$ {}^{1}w_1 = \begin{bmatrix} \cos\theta_1 & \sin\theta_1 & 0 \\ -\sin\theta_1 & \cos\theta_1 & 0 \\ 0 & 0 & 1 \end{bmatrix} \begin{bmatrix} 0 \\ 0 \\ 0 \end{bmatrix} + \dot{\theta}_1 \begin{bmatrix} 0 \\ 0 \\ 1 \end{bmatrix}$$

$$ {}^{1}w_1 = \begin{bmatrix} 0 \\ 0 \\ \dot{\theta}_1 \end{bmatrix} \tag{5.20}$$

- For i=0 linear velocity;

$$ {}^{0}v_0 = [0 \quad 0 \quad 0]^{T} \tag{5.21}$$

$$ {}^{1}v_1 = {}^{1}_{0}R({}^{0}v_0 + {}^{0}w_0 \times {}^{0}P_1) \tag{5.22}$$

$$ {}^{1}v_1 = \begin{bmatrix} \cos\theta_1 & \sin\theta_1 & 0 \\ -\sin\theta_1 & \cos\theta_1 & 0 \\ 0 & 0 & 1 \end{bmatrix} \left(\begin{bmatrix} 0 \\ 0 \\ 0 \end{bmatrix} + \begin{bmatrix} 0 \\ 0 \\ 0 \end{bmatrix} \times \begin{bmatrix} 0 \\ 0 \\ 0 \end{bmatrix} \right)$$

$$ {}^{1}v_1 = \begin{bmatrix} 0 \\ 0 \\ 0 \end{bmatrix} \tag{5.23}$$

- For i=1 angular velocity;

$$ {}^{2}w_2 = {}^{2}_{1}R\,{}^{1}w_1 + \dot{\theta}_2\,{}^{2}Z_2 \tag{5.24}$$

$$ {}^{2}w_2 = \begin{bmatrix} \cos\theta_2 & \sin\theta_2 & 0 \\ -\sin\theta_2 & \cos\theta_2 & 0 \\ 0 & 0 & 1 \end{bmatrix} \begin{bmatrix} 0 \\ 0 \\ \dot{\theta}_1 \end{bmatrix} + \dot{\theta}_2 \begin{bmatrix} 0 \\ 0 \\ 1 \end{bmatrix}$$

$$ {}^{2}w_2 = \begin{bmatrix} 0 \\ 0 \\ \dot{\theta}_1 + \dot{\theta}_2 \end{bmatrix} \tag{5.25}$$

- For i=1 linear velocity;

$$^{2}v_2 = {}^{2}_{1}\mathrm{R}(^{1}\mathrm{v}_1 + {}^{1}\mathrm{w}_1 \,\mathrm{x}\, {}^{1}\mathrm{P}_2) \tag{5.26}$$

$$^{2}v_2 = \begin{bmatrix} \cos\theta_2 & \sin\theta_2 & 0 \\ -\sin\theta_2 & \cos\theta_2 & 0 \\ 0 & 0 & 1 \end{bmatrix} \left(\begin{bmatrix} 0 \\ 0 \\ 0 \end{bmatrix} + \begin{bmatrix} 0 \\ 0 \\ \dot{\theta}_1 \end{bmatrix} \mathrm{x} \begin{bmatrix} 418{,}72 \\ -152{,}4 \\ 0 \end{bmatrix} \right)$$

$$^{2}v_2 = \begin{bmatrix} 152{,}4\cos\theta_2\dot{\theta}_1 + 418{,}72\sin\theta_2\,\dot{\theta}_1 \\ -152{,}4\sin\theta_2\dot{\theta}_1 + 418{,}72\cos\theta_2\dot{\theta}_1 \\ 0 \end{bmatrix} \tag{5.27}$$

- For i=2 angular velocity;

$$^{3}w_3 = {}^{3}_{2}\mathrm{R}\,{}^{2}w_2 + 0\,{}^{3}\mathrm{Z}_3 \tag{5.28}$$

$$^{3}w_3 = \begin{bmatrix} 1 & 0 & 0 \\ 0 & 1 & 0 \\ 0 & 0 & 1 \end{bmatrix} \begin{bmatrix} 0 \\ 0 \\ \dot{\theta}_1 + \dot{\theta}_2 \end{bmatrix}$$

$$^{3}w_3 = \begin{bmatrix} 0 \\ 0 \\ \dot{\theta}_1 + \dot{\theta}_2 \end{bmatrix} \tag{5.29}$$

- For i=2 linear velocity;

$$^{3}v_3 = {}^{3}_{2}\mathrm{R}(^{2}v_2 + {}^{2}w_2 \mathrm{x}\, {}^{2}\mathrm{P}_3) \tag{5.30}$$

$$^{3}\mathrm{v}_3 = \begin{bmatrix} (418{,}72\sin\theta_2 + 152{,}4\cos\theta_2 + 300)\,\dot{\theta}_1 + 300\,\dot{\theta}_2 \\ (-152{,}4\sin\theta_2 + 418{,}72\cos\theta_2)\,\dot{\theta}_1 \\ 0 \end{bmatrix} \tag{5.31}$$

- For i=3 angular velocity;

$$^{4}w_4 = {}^{4}_{3}\mathrm{R}\,{}^{3}w_3 + \dot{\theta}_3\,{}^{4}\mathrm{Z}_4 \tag{5.32}$$

$$^{4}w_4 = \begin{bmatrix} 0 & \sin\theta_3 & -\cos\theta_3 \\ 0 & \cos\theta_3 & \sin\theta_3 \\ 1 & 0 & 0 \end{bmatrix} \begin{bmatrix} 0 \\ 0 \\ \dot{\theta}_1 + \dot{\theta}_2 \end{bmatrix} + \dot{\theta}_3 \begin{bmatrix} 0 \\ 0 \\ 1 \end{bmatrix}$$

$$^{4}w_4 = \begin{bmatrix} -\cos\theta_3\dot{\theta}_1 - \cos\theta_3\dot{\theta}_2 \\ \sin\theta_3\,\dot{\theta}_1 + \sin\theta_3\,\dot{\theta}_2 \\ \dot{\theta}_3 \end{bmatrix} \tag{5.33}$$

- For i=3 linear velocity;

$$ {}^{4}v_4 = {}^{4}_{3}\mathrm{R}({}^{3}v_3 + {}^{3}w_3 \times {}^{3}\mathrm{P}_4) \tag{5.34}$$

$$ {}^{4}v_4 = \begin{bmatrix} (-152{,}4\sin\theta_2 \sin\theta_3 + 418{,}72\cos\theta_2 \sin\theta_3 + 724{,}28\sin\theta_3)\dot{\theta}_1 + 724{,}28\sin\theta_3\,\dot{\theta}_2 \\ (-152{,}4\sin\theta_2 \cos\theta_3 + 418{,}72\cos\theta_2\cos\theta_3 + 724{,}28\cos\theta_3)\,\dot{\theta}_1 + 724{,}28\cos\theta_3\,\dot{\theta}_2 \\ (418{,}72\sin\theta_2 + 152{,}4\cos\theta_2 + 150)\,\dot{\theta}_1 + 150\dot{\theta}_2 \end{bmatrix} \tag{5.35}$$

Forward kinematic transformation matrice multiplication of the system is;

$$ {}^{0}_{4}\mathrm{R} = {}^{0}_{1}\mathrm{R}\,{}^{1}_{2}\mathrm{R}\,{}^{2}_{3}\mathrm{R}\,{}^{3}_{4}\mathrm{R} = \begin{bmatrix} \cos\theta_1 & -\sin\theta_1 & 0 \\ \sin\theta_1 & \cos\theta_1 & 0 \\ 0 & 0 & 1 \end{bmatrix} \begin{bmatrix} \cos\theta_2 & -\sin\theta_2 & 0 \\ \sin\theta_2 & \cos\theta_2 & 0 \\ 0 & 0 & 1 \end{bmatrix} \begin{bmatrix} 1 & 0 & 0 \\ 0 & 1 & 0 \\ 0 & 0 & 1 \end{bmatrix} \begin{bmatrix} 0 & 0 & 1 \\ \sin\theta_3 & \cos\theta_3 & 0 \\ -\cos\theta_3 & \sin\theta_3 & 0 \end{bmatrix} \tag{5.36}$$

The linear velocity of the coordinate system 4 with respect to the base coordinate system 0 is obtained by the equation below;

$$ {}^{0}v_4 = {}^{0}_{4}\mathrm{R}\,{}^{4}v_4 \tag{5.37}$$

The angular velocity of the coordinate system 4 with respect to the base coordinate system 0 is obtained by the equation below;

$$ {}^{0}w_4 = {}^{0}_{4}\mathrm{R}\,{}^{4}w_4 \tag{5.38}$$

Jacobian matrice of the system is obtained by linear and angular velocity;

$$ {}^{0}v_4 = \mathrm{J}_v(\theta)\dot{\theta} \tag{5.39}$$

$$ {}^{0}w_4 = \mathrm{J}_w(\theta)\dot{\theta} \tag{5.40}$$

CHAPTER SIX
DYNAMIC SYSTEM MODELING

Individual center of gravity position of every link is determined with respect to own reference coordinate system on it. Torques are calculated effecting to the link joints. Figure 6.1 shows the system model and Table 6.1 shows the inertial properties.

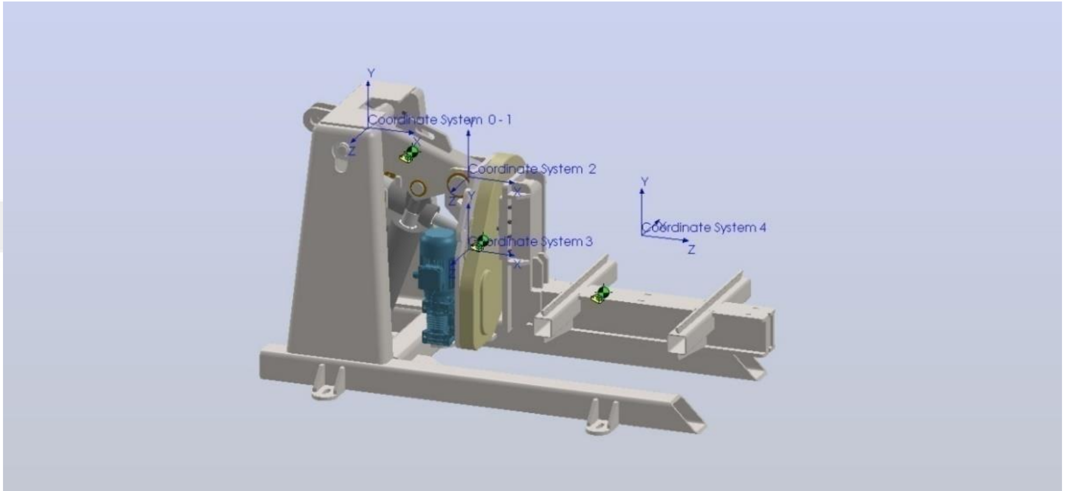

Figure 6.1 System modeling

Table 6.1 Inertial properties and center of gravity positions

Inertial Properties	Member Link A	Member Link B	Member End
Origin[a]	$[0 \quad 0 \quad 0]^T$	$[418.72 \quad -152.40 \quad 0]^T$	$[1143 \quad -302.40 \quad 0]^T$
Center of Gravity[b] P_C	$[185.51 \quad -78.61 \quad 0]^T$	$[73.47 \quad -250.09 \quad 96.14]^T$	$[0 \quad -206.47 \quad -238.21]^T$
Mass [kg]	50.04	115.51	168.25
$\mathbf{I_G}$[c] **Inertial Tensor**	$\begin{bmatrix} 0.48 & -0.05 & 0 \\ -0.05 & 2.04 & 0 \\ 0 & 0 & 1.81 \end{bmatrix}$	$\begin{bmatrix} 6.88 & 0.15 & -0.19 \\ 0.15 & 3.89 & -1.07 \\ -0.19 & -1.07 & 3.60 \end{bmatrix}$	$\begin{bmatrix} 6.79 & -6.13 & 0 \\ -6.13 & 22.06 & 0 \\ 0 & 0 & 25.41 \end{bmatrix}$

a; Local origin position respect to base coordinate system [mm]
b; Center of gravity position respect to local origin [mm]
c; Inertial moment respect to center of gravity [kg-m²]

$$^{0}w_0 = [0 \quad 0 \quad 0]^T \tag{6.1}$$

$$^{0}\dot{w}_0 = [0 \quad 0 \quad 0]^T \tag{6.2}$$

$$^{0}\dot{v}_0 = g[0 \quad 1 \quad 0]^T \tag{6.3}$$

$$^{i+1}_{\ \ i}R = {}^{\ \ \ i}_{i+1}R^T \tag{6.4}$$

1) Determining forward kinetic equations for Member Link A;

Angular velocity for the first link;

$$ {}^{1}w_1 = {}^{1}_{0}R\,{}^{0}w_0 + \dot{\theta}_1\,{}^{1}Z_1 \tag{6.5} $$

$$ {}^{1}w_1 = [0 \quad 0 \quad \dot{\theta}_1]^T \tag{6.6} $$

Angular acceleration for the first link;

$$ {}^{1}\dot{w}_1 = {}^{1}_{0}R\,{}^{0}\dot{w}_0 + \ddot{\theta}_1\,{}^{1}Z_1 + {}^{1}_{0}R\,{}^{0}w_0 x \dot{\theta}_1\,{}^{1}Z_1 \tag{6.7} $$

$$ {}^{1}\dot{w}_1 = [0 \quad 0 \quad \ddot{\theta}_1]^T \tag{6.8} $$

Linear acceleration for the first link;

$$ {}^{1}\dot{v}_1 = {}^{1}_{0}R({}^{0}\dot{w}_0 x\,{}^{0}P_1 + {}^{0}w_0 x[{}^{0}w_0 x\,{}^{0}P_1] + {}^{0}\dot{v}_0) \tag{6.9} $$

$$ {}^{1}\dot{v}_1 = \begin{bmatrix} g\sin\theta_1 \\ g\cos\theta_1 \\ 0 \end{bmatrix} \tag{6.10} $$

Linear acceleration of the center of gravity for the first link;

$$ {}^{1}\dot{v}_{C_1} = {}^{1}\dot{w}_1 x\,{}^{1}P_{C_1} + {}^{1}w_1 x[{}^{1}w_1 x\,{}^{1}P_{C_1}] + {}^{1}\dot{v}_1 \tag{6.11} $$

$$ {}^{1}\dot{v}_{C_1} = \begin{bmatrix} 0.07861\ddot{\theta}_1 - 0.18551\dot{\theta}_1^{\,2} + g\sin\theta_1 \\ 0.18551\ddot{\theta}_1 + 0.07861\dot{\theta}_1^{\,2} + g\cos\theta_1 \\ 0 \end{bmatrix} \tag{6.12} $$

Force vector for the first link;

$$ {}^{1}F_1 = m_1\,{}^{1}\dot{v}_{C_1} \tag{6.13} $$

$$ {}^{1}F_1 = \begin{bmatrix} 3.934\ddot{\theta}_1 - 9.283\dot{\theta}_1^{\,2} + 50.04g\sin\theta_1 \\ 9.283\ddot{\theta}_1 + 3.934\dot{\theta}_1^{\,2} + 50.04g\cos\theta_1 \\ 0 \end{bmatrix} \left[\frac{kg-m}{s^2}\right] \tag{6.14} $$

Moment vector for the first link;

$$ {}^{1}N_1 = {}^{1}I_{C1}\,{}^{1}\dot{w}_1 + {}^{1}w_1 x({}^{1}I_{C1}\,{}^{1}w_1) \tag{6.15} $$

$$^{1}N_1 = \begin{bmatrix} 0 \\ 0 \\ 1.81\ddot{\theta}_1 \end{bmatrix} \tag{6.16}$$

2) Determining the forward kinetic equations for Member Link B;

Angular velocity for the second link;

$$^{2}w_2 = {}^{2}_{1}R\,{}^{1}w_1 + \dot{\theta}_2\,{}^{2}Z_2 \tag{6.17}$$

$$^{2}w_2 = \begin{bmatrix} 0 \\ 0 \\ \dot{\theta}_1 + \dot{\theta}_2 \end{bmatrix} \tag{6.18}$$

Angular acceleration for the second link;

$$^{2}\dot{w}_2 = {}^{2}_{1}R\,{}^{1}\dot{w}_1 + \ddot{\theta}_2\,{}^{2}Z_2 + {}^{2}_{1}R\,{}^{1}w_1 x \dot{\theta}_2\,{}^{2}Z_2 \tag{6.19}$$

$$^{2}\dot{w}_2 = \begin{bmatrix} 0 \\ 0 \\ \ddot{\theta}_1 + \ddot{\theta}_2 \end{bmatrix} \tag{6.20}$$

Linear acceleration for the second link;

$$^{2}\dot{v}_2 = {}^{2}_{1}R({}^{1}\dot{w}_1 x\,{}^{1}P_2 + {}^{1}w_1 x[{}^{1}w_1 x\,{}^{1}P_2] + {}^{1}\dot{v}_1) \tag{6.21}$$

$$^{2}\dot{v}_2 = \begin{bmatrix} \cos\theta_2(0.1524\ddot{\theta}_1 - 0.41872\dot{\theta}_1{}^2 + g\sin\theta_1) + \sin\theta_2(0.41872\ddot{\theta}_1 - 0.1524\dot{\theta}_1{}^2 + g\cos\theta_1) \\ \cos\theta_2(0.41872\ddot{\theta}_1 + 0.1524\dot{\theta}_1{}^2 + g\cos\theta_1) - \sin\theta_2\,(0.1524\ddot{\theta}_1 - 0.41872\dot{\theta}_1{}^2 + g\sin\theta_1) \\ 0 \end{bmatrix} \tag{6.22}$$

Linear acceleration of the center of gravity for the second link;

$$^{2}\dot{v}_{C_2} = {}^{2}\dot{w}_2 x\,{}^{2}P_{C_2} + {}^{2}w_2 x[{}^{2}w_2 x\,{}^{2}P_{C_2}] + {}^{2}\dot{v}_2 \tag{6.23}$$

$$^{2}\dot{v}_{C_2} = \begin{bmatrix} \dot{v}_{C_{2x}} \\ \dot{v}_{C_{2y}} \\ \dot{v}_{C_{2z}} \end{bmatrix}$$

Force vector for the second link;

$$^{2}F_2 = m_2\,{}^{2}\dot{v}_{C_2} \tag{6.24}$$

$$^2F_2 = \begin{bmatrix} F_{2_x} \\ F_{2_y} \\ F_{2_z} \end{bmatrix}$$

Moment vector for the second link;

$$^2N_2 = {^2I_{C_2}}\,{^2\dot{w}_2} + {^2w_2}x({^2I_{C_2}}\,{^2w_2}) \tag{6.25}$$

$$^2N_2 = \begin{bmatrix} 1.07[\dot{\theta}_1 + \dot{\theta}_2]^2 - 0.19[\ddot{\theta}_1 + \ddot{\theta}_2] \\ -0.19[\dot{\theta}_1 + \dot{\theta}_2]^2 - 1.07[\ddot{\theta}_1 + \ddot{\theta}_2] \\ 3.60[\ddot{\theta}_1 + \ddot{\theta}_2] \end{bmatrix} \tag{6.26}$$

3) Determining the forward kinetic equations for Member End;

Angular velocity for the third link;

$$^3w_3 = {}^4_2R\,{^2w_2} + \dot{\theta}_3\,{^3Z_3} \tag{6.27}$$

$$^3w_3 = \begin{bmatrix} -\cos\theta_3[\dot{\theta}_1 + \dot{\theta}_2] \\ \sin\theta_3\,[\dot{\theta}_1 + \dot{\theta}_2] \\ \dot{\theta}_3 \end{bmatrix} \tag{6.28}$$

Angular acceleration for the third link;

$$^3\dot{w}_3 = {}^4_2R\,{^2\dot{w}_2} + \ddot{\theta}_3\,{^3Z_3} + {}^4_2R\,{^2w_2}x\dot{\theta}_3\,{^3Z_3} \tag{6.29}$$

$$^3\dot{w}_3 = \begin{bmatrix} \sin\theta_3\,[\dot{\theta}_1 + \dot{\theta}_2]\dot{\theta}_3 - \cos\theta_3[\ddot{\theta}_1 + \ddot{\theta}_2] \\ \cos\theta_3[\dot{\theta}_1 + \dot{\theta}_2]\,\dot{\theta}_3 + \sin\theta_3[\ddot{\theta}_1 + \ddot{\theta}_2] \\ \ddot{\theta}_3 \end{bmatrix} \tag{6.30}$$

Linear acceleration for the third link;

$$^3\dot{v}_3 = {}^4_2R({^2\dot{w}_2}x{^2P_4} + {^2w_2}x[{^2w_2}x{^2P_4}] + {^2\dot{v}_2}) \tag{6.31}$$

$$^3\dot{v}_3 = \begin{bmatrix} \dot{v}_{3_x} \\ \dot{v}_{3_y} \\ \dot{v}_{3_z} \end{bmatrix} \tag{6.32}$$

Linear acceleration of the center of gravity for the third link;

$$^{3}\dot{v}_{C_3} = {}^{3}\dot{w}_3 x^{3}P_{C_3} + {}^{3}w_3 x[^{3}w_3 x^{3}P_{C_3}] + {}^{3}\dot{v}_3 \tag{6.33}$$

$$^{3}\dot{v}_{C_3} = \begin{bmatrix} \dot{v}_{C_{3x}} \\ \dot{v}_{C_{3y}} \\ \dot{v}_{C_{3z}} \end{bmatrix} \tag{6.34}$$

Force vector for the third link;

$$^{3}F_3 = m_3 {}^{3}\dot{v}_{C_3} \tag{6.35}$$

$$^{3}F_3 = \begin{bmatrix} F_{3_x} \\ F_{3_y} \\ F_{3_z} \end{bmatrix} \tag{6.36}$$

Moment vector for the third link;

$$^{3}N_3 = {}^{3}I_{C_3} {}^{3}\dot{w}_3 + {}^{3}w_3 x\left({}^{3}I_{C_3} {}^{3}w_3\right) \tag{6.37}$$

$$^{3}N_3 = \begin{bmatrix} N_{3_x} \\ N_{3_y} \\ N_{3_z} \end{bmatrix} \tag{6.38}$$

Calculation of the forces and torques acting on the link joints;

1) Force acting on the third link joint;

$$^{3}f_3 = {}^{4}_{5}R^{5}f_5 + {}^{3}F_3 \tag{6.39}$$

$$^{3}f_3 = {}^{4}_{5}R^{5}f_5 + m_3 {}^{3}\dot{v}_{C_3}$$

$$^{3}f_3 = \begin{bmatrix} ^{3}f_{3x} \\ ^{3}f_{3y} \\ ^{3}f_{3z} \end{bmatrix}$$

- Torque acting on the third link joint;

$$^{3}n_3 = {}^{3}N_3 + {}^{4}_{5}R\,{}^{5}n_5 + {}^{3}P_{C_3} x\, {}^{3}F_3 + {}^{4}P_5 x\, {}^{4}_{5}R\,{}^{5}f_5 \tag{6.40}$$

$$^{3}n_3 = {}^{3}N_3 + {}^{3}P_{C_3} x\, {}^{3}F_3$$

$$^{3}n_3 = \begin{bmatrix} {}^{3}n_{3x} \\ {}^{3}n_{3y} \\ {}^{3}n_{3z} \end{bmatrix} \tag{6.41}$$

2) Force acting on the second link joint;

$$^{2}f_2 = {}^{2}_{4}R\,{}^{3}f_3 + {}^{2}F_2 \tag{6.42}$$

$$^{2}f_2 = \begin{bmatrix} {}^{2}f_{2x} \\ {}^{2}f_{2y} \\ {}^{2}f_{2z} \end{bmatrix} \tag{6.43}$$

- Torque acting on the second link joint;

$$^{2}n_2 = {}^{2}N_2 + {}^{2}_{4}R\,{}^{3}n_3 + {}^{2}P_{C_2} x\, {}^{2}F_2 + {}^{2}P_4 x\, {}^{2}_{4}R\,{}^{3}f_3 \tag{6.44}$$

$$^{2}n_2 = \begin{bmatrix} {}^{2}n_{2x} \\ {}^{2}n_{2y} \\ {}^{2}n_{2z} \end{bmatrix} \tag{6.45}$$

3) Force acting on the first link joint;

$$^{1}f_1 = {}^{1}_{2}R\,{}^{2}f_2 + {}^{1}F_1 \tag{6.46}$$

$$^{1}f_1 = \begin{bmatrix} {}^{1}f_{1x} \\ {}^{1}f_{1y} \\ {}^{1}f_{1z} \end{bmatrix} \tag{6.47}$$

- Torque acting on the first link joint;

$$^{1}n_1 = {}^{1}N_1 + {}^{1}_{2}R\,{}^{2}n_2 + {}^{1}P_{C_1} x\, {}^{1}F_1 + {}^{1}P_2 x\, {}^{1}_{2}R\,{}^{2}f_2 \tag{6.48}$$

$$ {}^{1}n_1 = \begin{bmatrix} {}^{1}n_{1x} \\ {}^{1}n_{1y} \\ {}^{1}n_{1z} \end{bmatrix} \tag{6.49} $$

- Torque acting on the individual links;

$$ \tau_i = {}^{i}n_i^{T}\ {}^{i}Z_i \tag{6.50} $$

$$ \tau_1 = {}^{1}n_1^{T}\ {}^{1}Z_1 = {}^{1}n_1^{T}[0 \quad 0 \quad 1]^{T} \tag{6.51} $$

$$ \tau_2 = {}^{2}n_2^{T}\ {}^{2}Z_2 = \tau_2 = {}^{2}n_2^{T}[0 \quad 0 \quad 1]^{T} \tag{6.52} $$

$$ \tau_3 = {}^{3}n_3^{T}\ {}^{3}Z_3 = {}^{3}n_3^{T}[0 \quad 0 \quad 1]^{T} \tag{6.53} $$

$$ \tau_1 = {}^{1}n_{1z} = 1.81\ddot{\theta}_1 + n_{2z} + 0.18551F_{1y} + 0.07861F_{1x} + 0.41872(\sin\theta_2 f_{2x} + \cos\theta_2 f_{2y}) + 0.1524(\cos\theta_2 f_{2x} - \sin\theta_2 f_{2y}) \tag{6.54} $$

$$ \tau_2 = 3.6[\ddot{\theta}_1 + \ddot{\theta}_2] + \sin\theta_3 n_{3y} - \cos\theta_3 n_{3x} + 0.25009F_{2x} + 0.07347F_{2y} + 0.72428(\sin\theta_3 f_{3x} + \cos\theta_3 f_{3y}) + 0.15f_{3z} \tag{6.55} $$

$$ \tau_3 = n_{3z} = N_{3_z} + 0.20647F_{3_x} \tag{6.56} $$

CHAPTER SEVEN
CASE STUDY

First of all, welding geometries with different sizes and orientation are determined on the workpiece working envelope and kinematic and kinetic calculations are handled. Also, time histories are calculated while the system is performing different weld tasks.

As a welding geometry orinetation criteria, calculations are handled with respect to the weld seams are considered parallel to the horizontal plane and welding gun is perpendicular to the normal vector of the welding seam.

Some spesific welding seam orientation organizations are performed and multiple weld tasks are calculated with respect to the welding speed, welding geometry position angles and welding seam length.

MIG/MAG and TIG arc welding applications are considered between the welding applications and ABB IRB 1660 ID six axis welding robot is used for the welding performances. This robot has 1.55 m reachability and 0.02 mm position repeatable accuracy and 6 kg payload. On the other hand, 80 mm/sec welding speed is determined for the performance tasks.

While the system is performing different welding tasks, kinematic-kinetic-motion planning integrated system design algorithm is studied to perform the entire system. Hydraulic system design is constructed as a result of kinematic-kinetic calculations and maximum velocities of the hydraulic actuators are calculated and system modeling design and flow chart are done.

Figure 7.1 illustrates the flow chart for the integrated system modeling approach and Figure 7.2 shows the hydraulic system flow chart respectively.

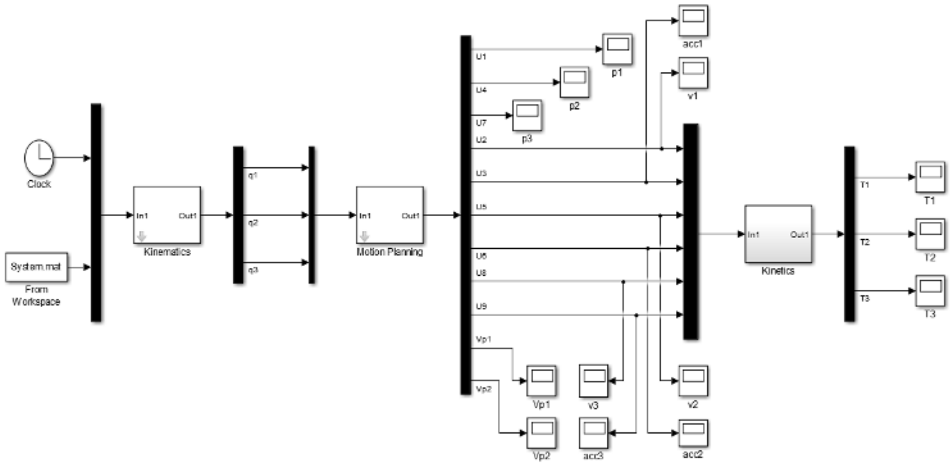

Figure 7.1 Integrated design algorithm

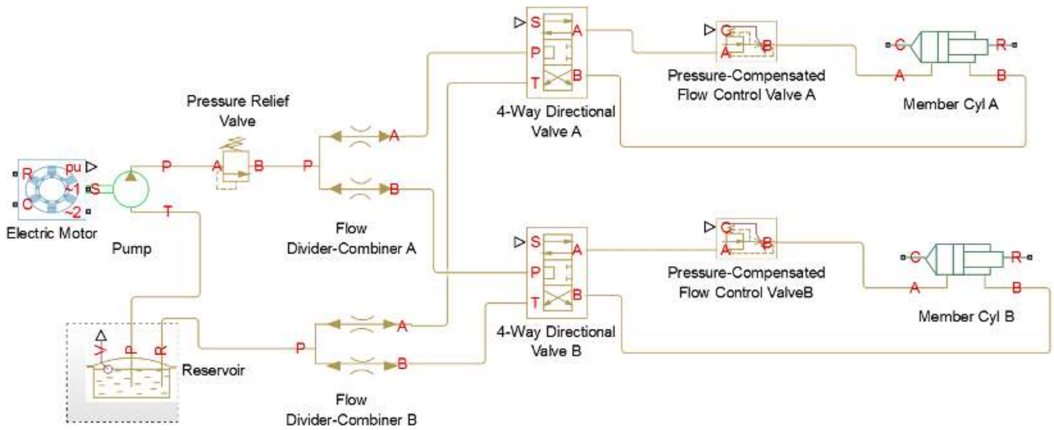

Figure 7.2 Hydraulic system flow chart

7.1 Welding Process

Welding process is performed via starting from the nearest region to the workpiece downside and positioner output table.

Kinematic solution for the system is obtained via the orthogonality of the system and z axis is assumed the approaching direction for welding applications. Kinematic solution of the welding orientation of the system;

$$ {}^{1}_{2}T\,{}^{2}_{3}T\,{}^{3}_{4}T\,{}^{4}_{5}W = {}^{0}_{5}W[{}^{0}_{1}T]^{-1} \tag{7.1}$$

When the system is considered respect to the joint space efficiency for the welding orientation, the angle θ_1 contributes the gaining height of the workpiece from the top plane, angle θ_2 can be adopted as slope angle of the weld seam horizontal orientation angle and θ_3 can be accepted as roll angle for the welding orientation.

7.2 Performance Tasks

The system is reviewed with respect to different performance tasks and welding conditions. Also, maximum velocities of the links are determined and kinematic – kinetic analysis is accomplished. Analysis results are obtained via calculation methods in Chapter 2.4 and Chapter 5 developed in this study. Table 7.1 shows the orientation angles, welding speeds, welding seam lengths and actuator displacements.

Table 7.1 Welding process parameters

Process	**Welding Speed**	**Seam Length**	**Actuator**	**Link Angle** $\theta_1; \theta_2; \theta_3$	**Displacement** $r_1; r_2; \theta_m$
Weld Path 1	60 mm/sec	240 mm	Cyl B	0° ; 15° ; 0°	0; 70.73; 0
Weld Path 2	30 mm/sec	338 mm	Motor	0° ; 0°; 45°	0; 0; 506.25°
Weld Path 3	30 mm/sec	240 mm	Cyl A - Cyl B	20° ;-35° ; 0°	104.58; -78.23; 0
Weld Path 4	30 mm/sec	180 mm	Cyl A – Cyl B	45°; -40°; 0°	234.91; -80.43; 0
Weld Path 5	40 mm/sec	160 mm	Cyl A –B -M	20°; 5°; 45°	104.58; 127.47; 506.25°
Weld Path 6	35 mm/sec	140 mm	Motor	0°; 0°; -60°	0; 0; -675°
Weld Path 7	40 mm/sec	236 mm	Cyl B - Motor	0°; 25°; 90°	0; 113.89; 1012.5°
Weld Path 8	80 mm/sec	536 mm	Cyl B	0°; 25°; 0°	0; 113.89; 0
Weld Path 9	40 mm/sec	358 mm	Cyl A – Cyl B	40°; -40°; 0°	209.85; -86.43; 0

Different weld path orientations are considered and a welding workspace is created for different performance tasks. Figure 7.3 shows the entire weld paths on the workpiece workspace.

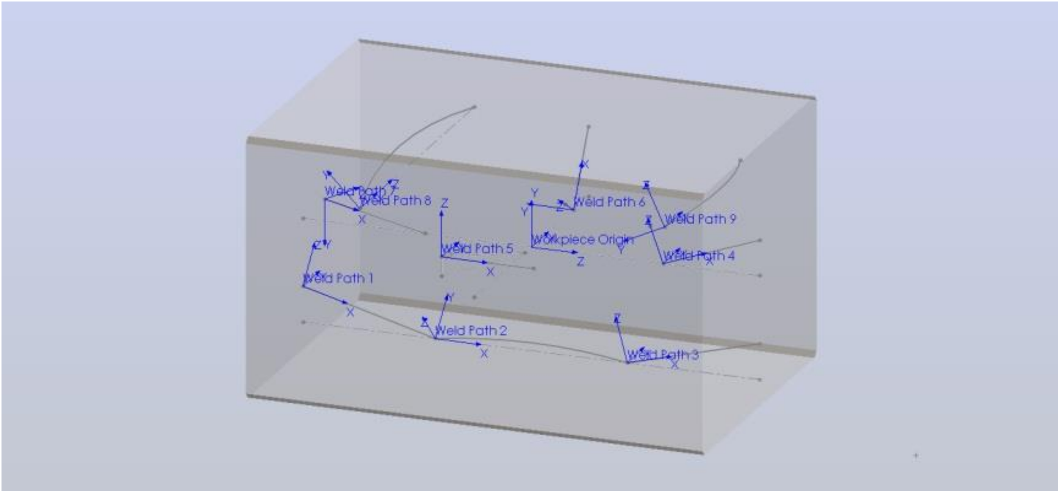

Figure 7.3 Welding orientations

Weld Path 1
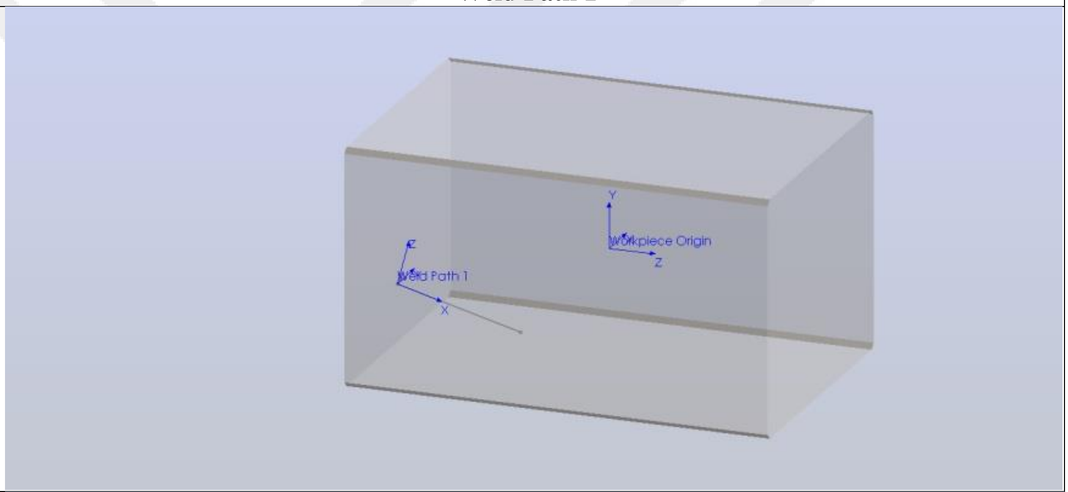
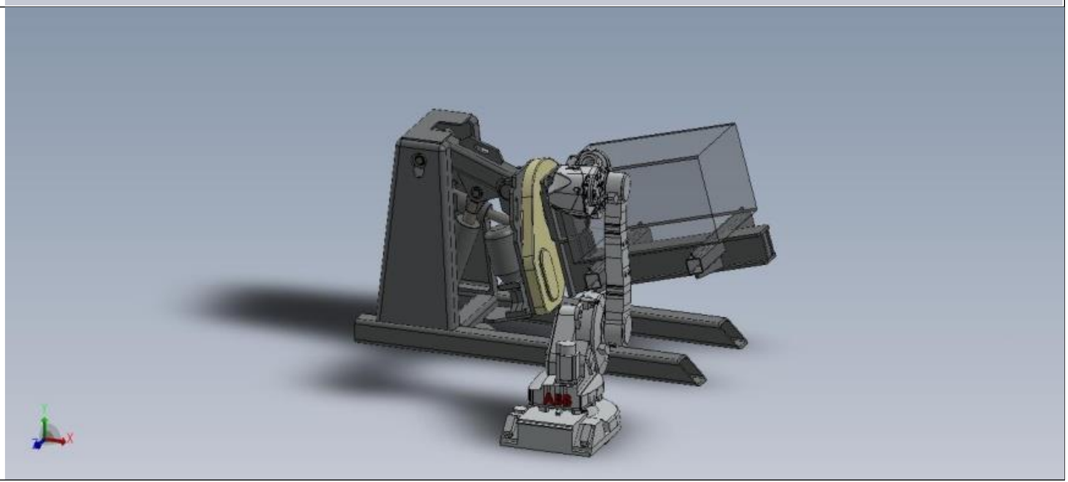

Figure 7.4 Weld path 1

Weld Path 2
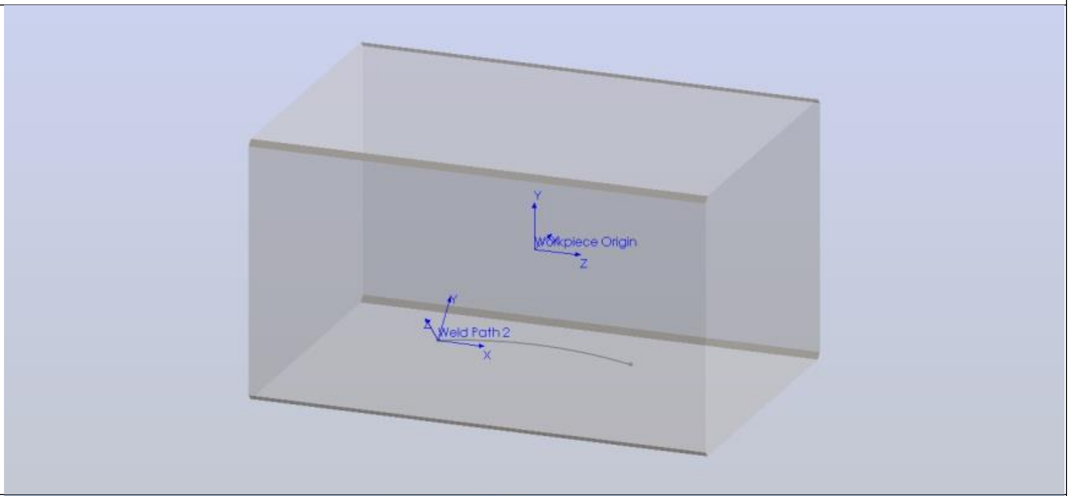
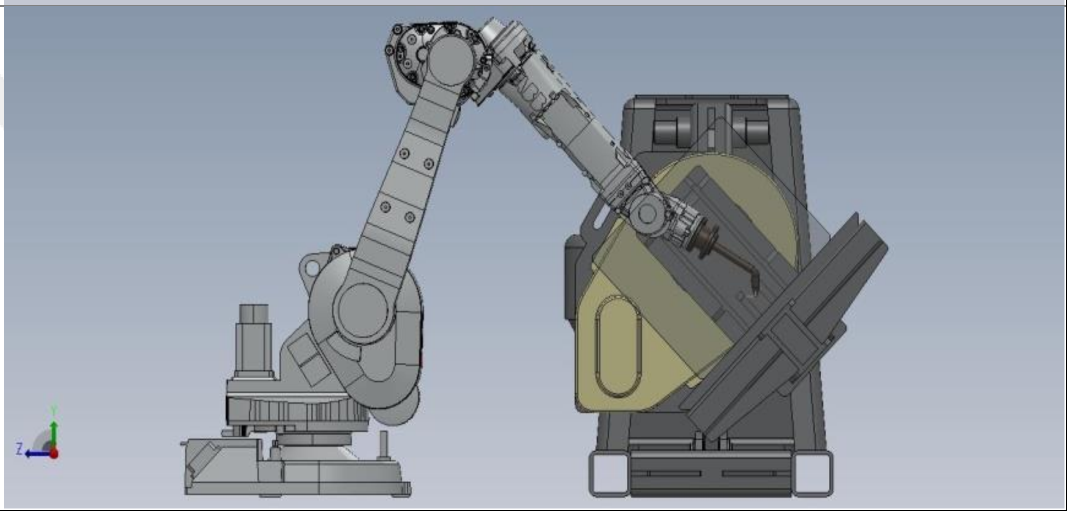

Figure 7.5 Weld path 2

Weld Path 3
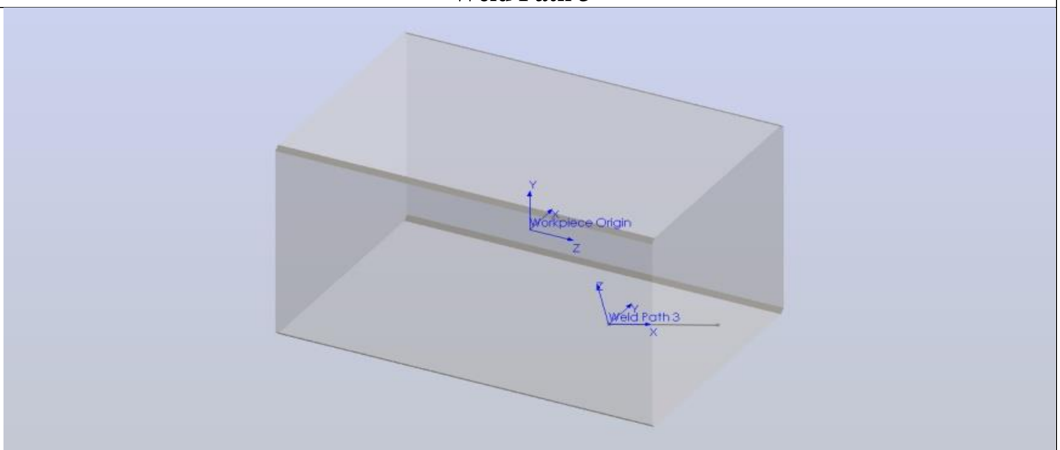
Figure 7.6 Weld path 3

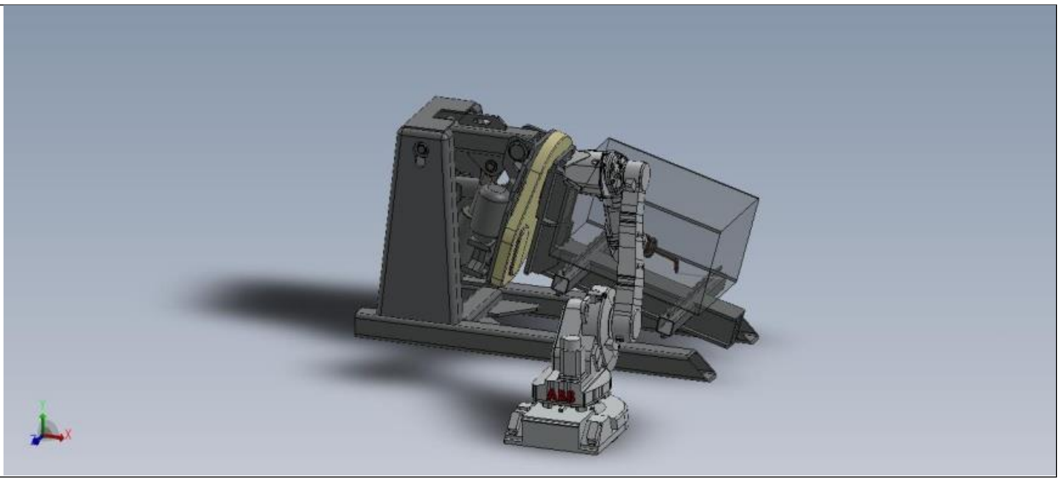

Figure 7.6 Weld path 3 (continue)

Weld Path 4

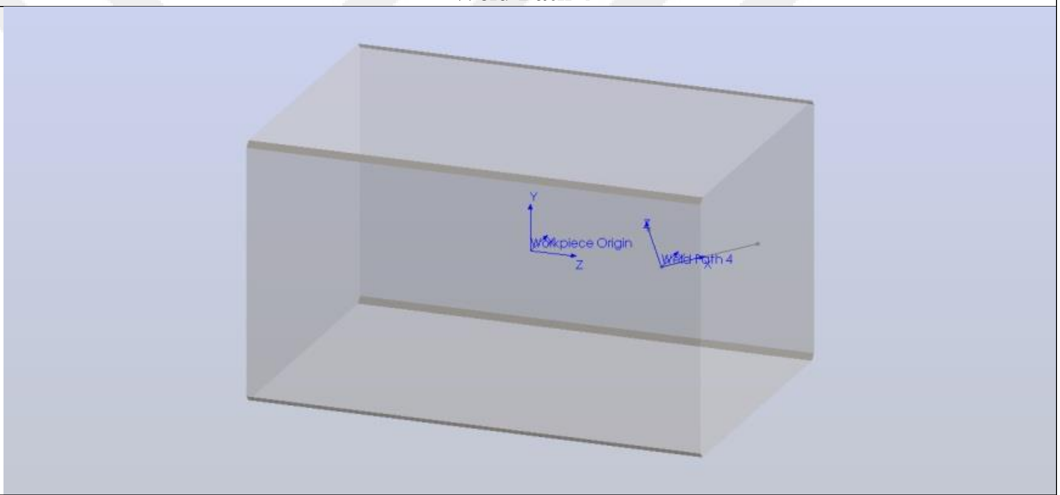

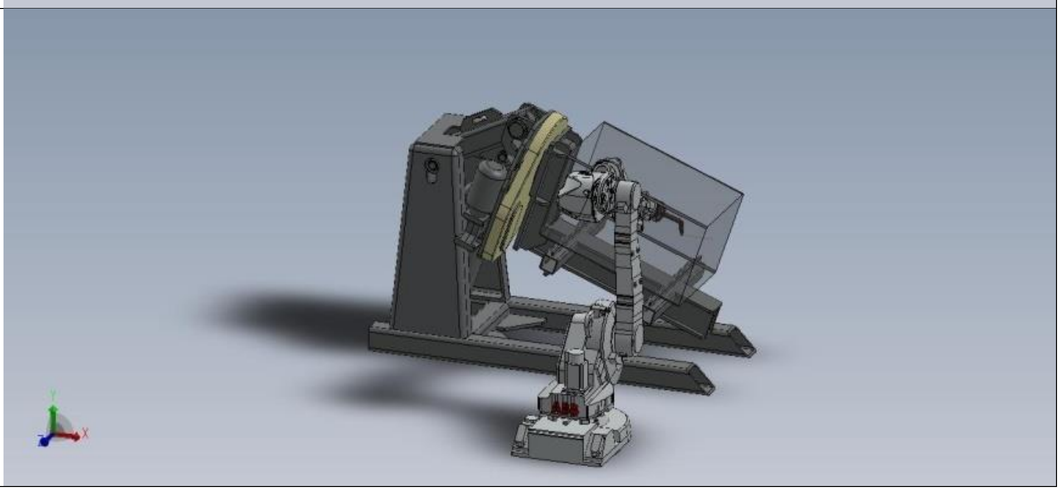

Figure 7.7 Weld path 4

Weld Path 5
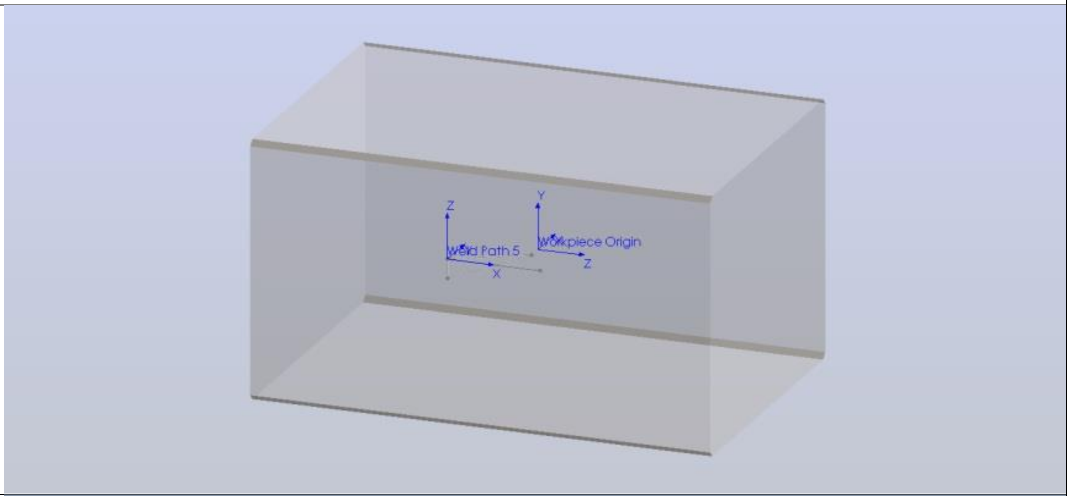
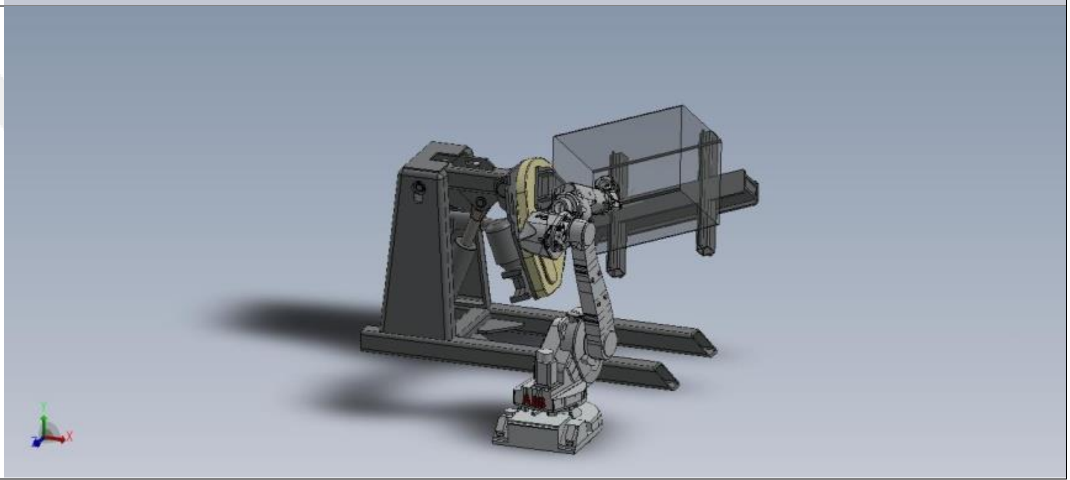

Figure 7.8 Weld path 5

While the system is performing weld path 5, actuator forces belong to Member Cyl A and Member Cyl B; F_1 and F_2 forces are obtained in the graphs. Also, actuator torque belongs to Member End is shown in the graphs. Table 7.2 shows the analysis results.

While the system is starting the motion $q_{E_0} = [1143;\ -302.40; 0]$ and the final position of the end point of the system $q_{E_1} = [1165.40;\ 170.15; 0]$ are obtained from the Cad model. $q_E = [1165.40;\ 170.15; 506.25°]$ can be calculated and the system outputs $q_A = [104.58; 127.47; 506.25°]$ are obtained from the calculations.

Table 7.2 Analysis results

Analysis Results		Weld Path 5
$q_E = [P_x;\ P_y;\ \theta_m]$	[mm; mm ; deg]	[1165.40; 170.15; 506.25°]
$q_{A^*} = [r_1;\ r_2;\ \theta_m]$	[mm; mm ; deg]	[99.34; 129.764; 506.25°]
$q_A = [r_1;\ r_2;\ \theta_m]$	[mm; mm ; deg]	[104.58; 127.47; 506.25°]
$q_V = [Q_1;\ Q_2;\ v_3]$	[lt/min; lt/min ; °/s]	[5.94; 3.83; 50.625]
$q_F = [F_1;\ F_2;\ T_m]$	[N; N ; Nm]	[26943; 35203; 90]
$q_P = [P_1;\ P_2;\ T_m]$	[bar; bar ; Nm]	[28.4; 70; 90]

q_{A^*}; Analytical calculation results of actuator displacements developed in this study
q_A ; Solidworks analysis results of actuator displacements
q_V ; Pump flow rates and electric motor velocity
q_F ; Actuator forces and electric motor torque
q_P ; Pressures and electric motor torque

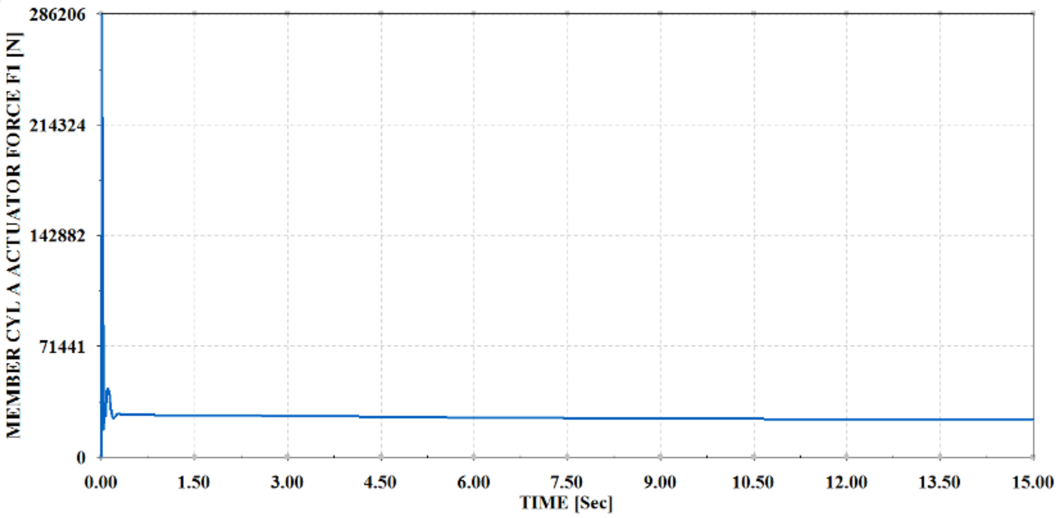

Figure 7.9 Member cyl A force

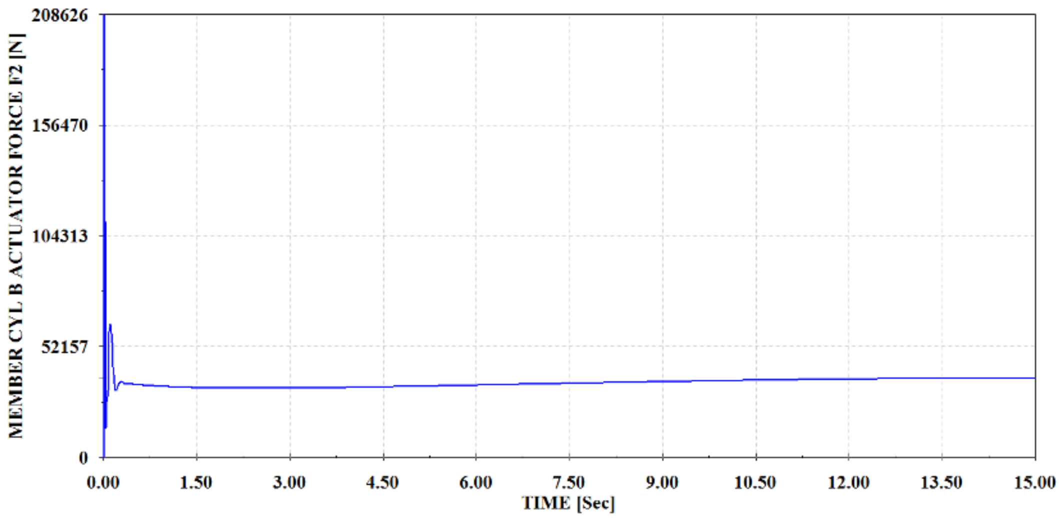

Figure 7.10 Member cyl B force

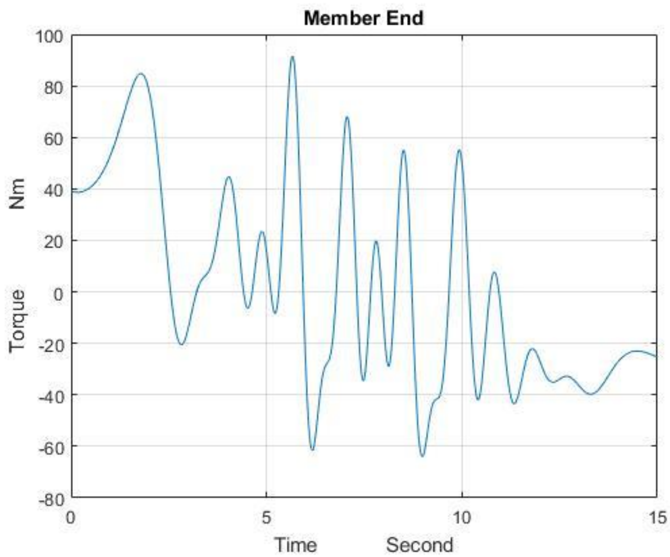

Figure 7.11 Member end actuator torque

Weld Path 6
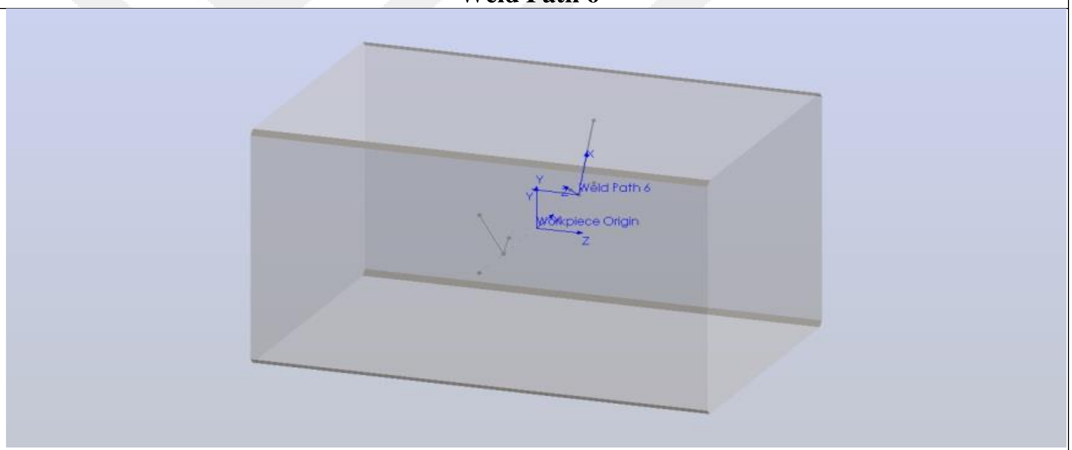
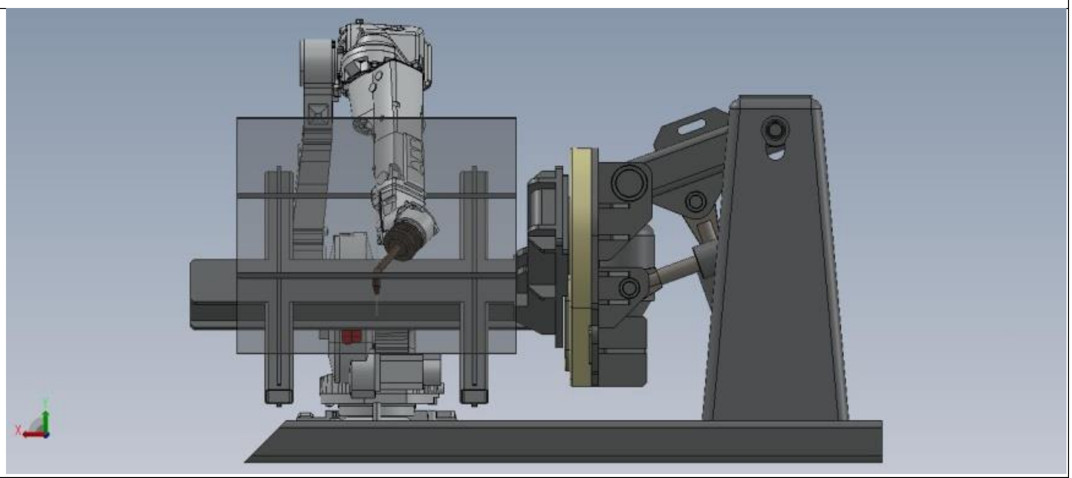

Figure 7.12 Weld path 6

Weld Path 7

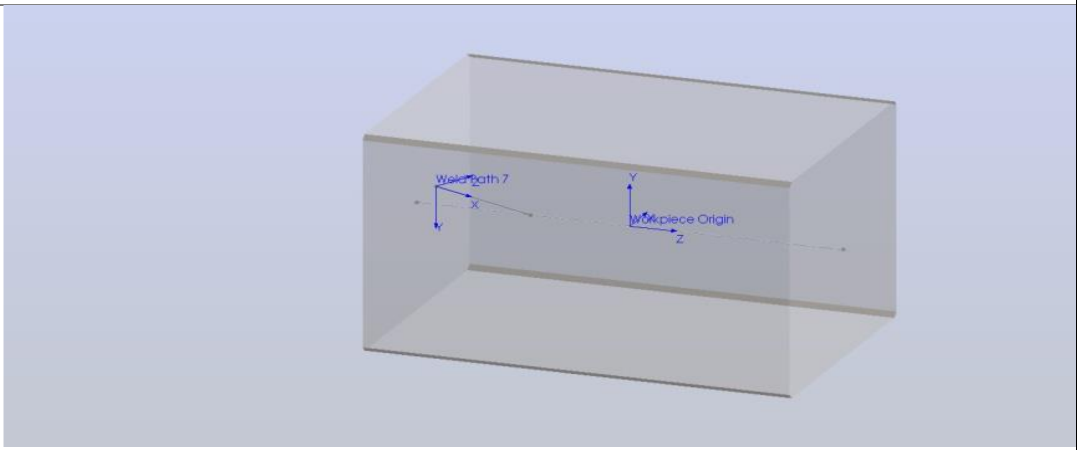

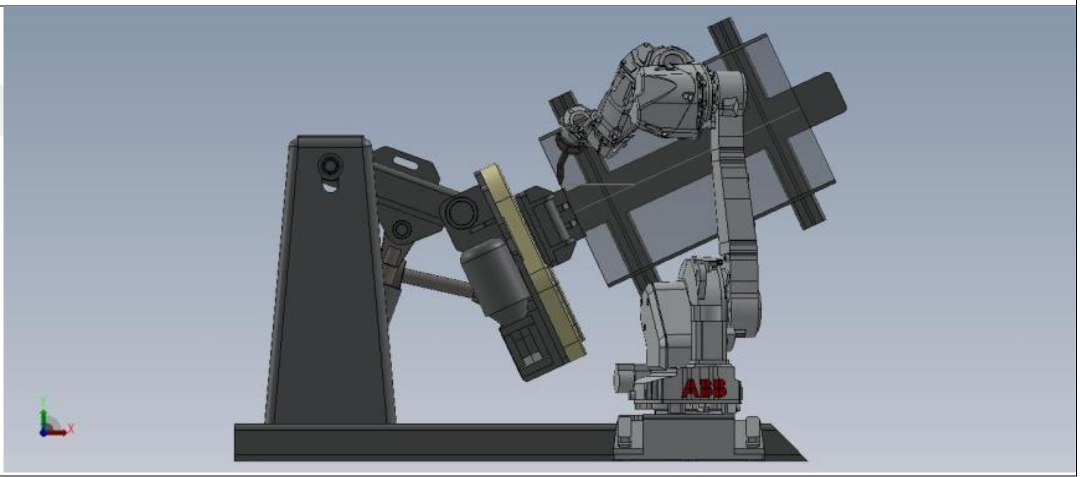

Figure 7.13 Weld path 7

Weld Path 8

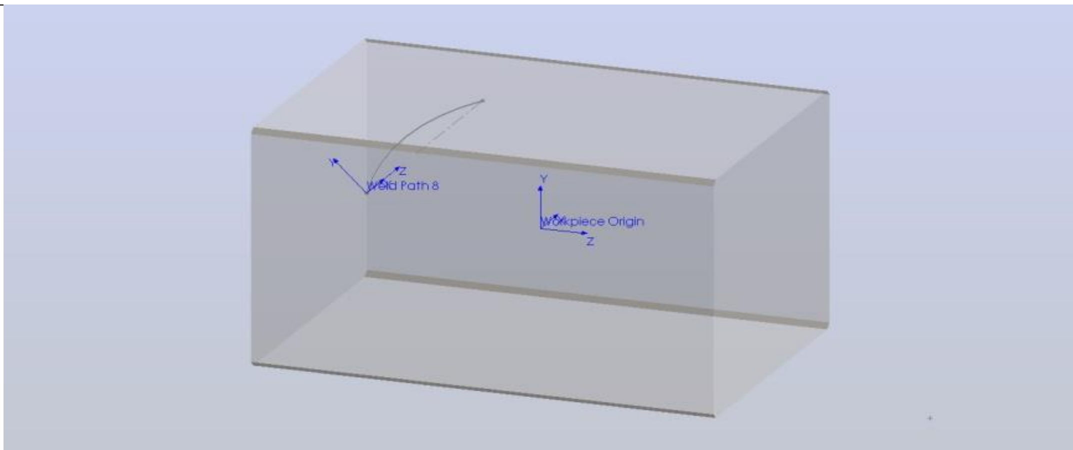

Figure 7.14 Weld path 8

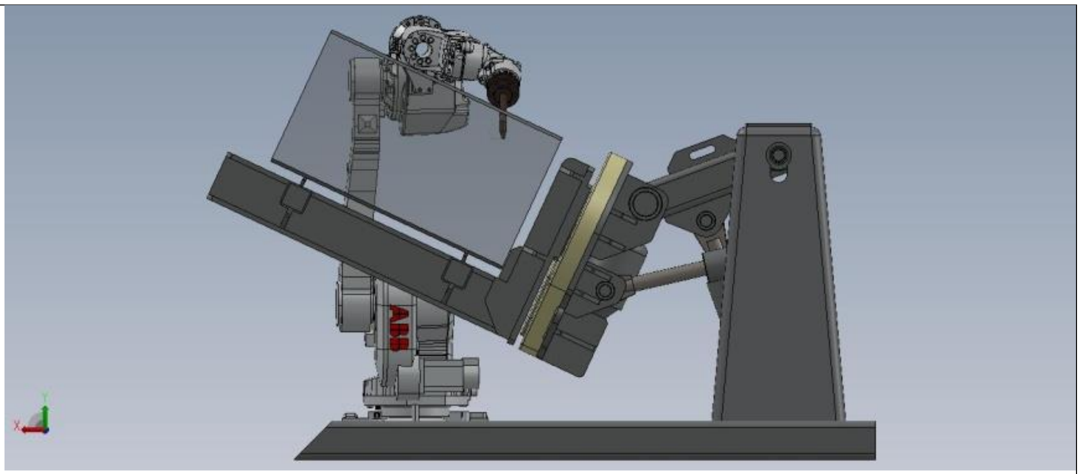

Figure 7.14 Weld path 8 (continue)

Weld Path 9

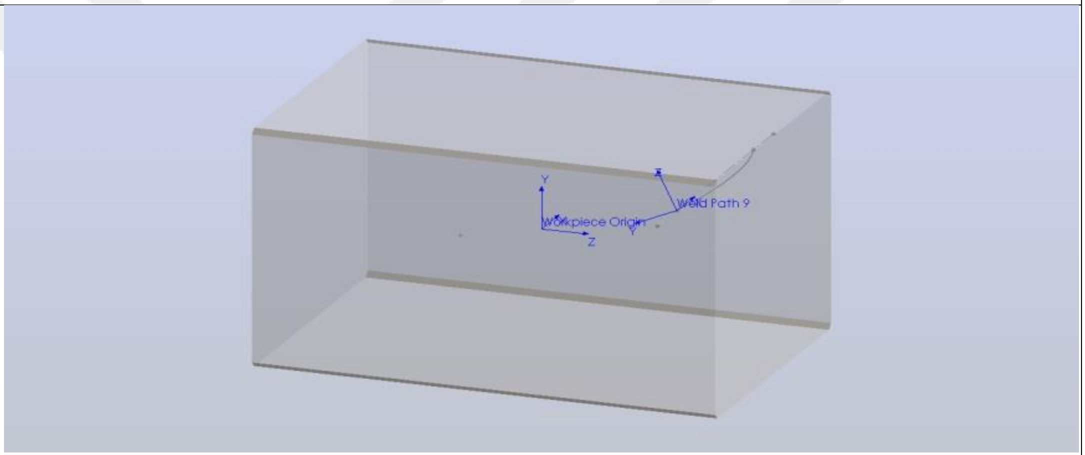

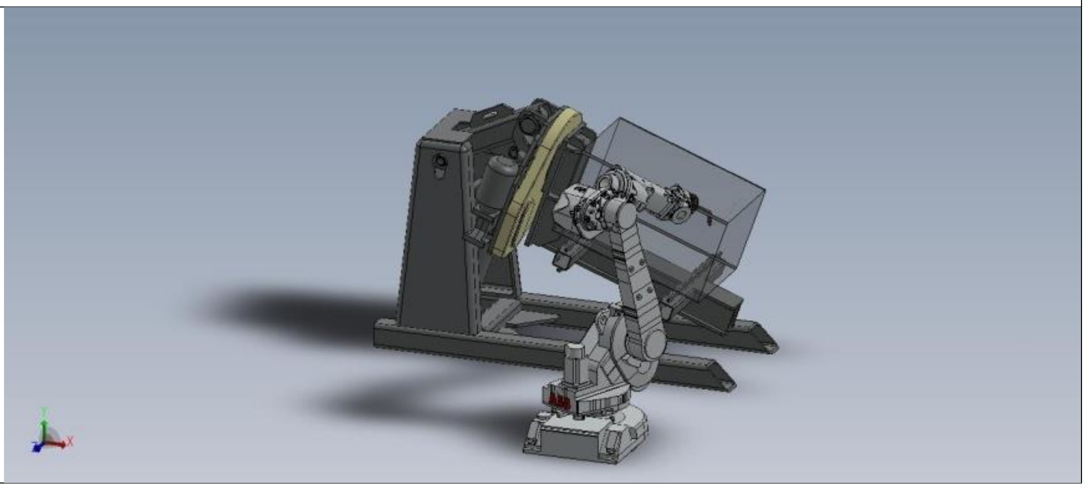

Figure 7.15 Weld path 9

Weld path 5 perfromance task is analyzed and reviewed for motion planning and time history studies and graphs are shown in the figures below.

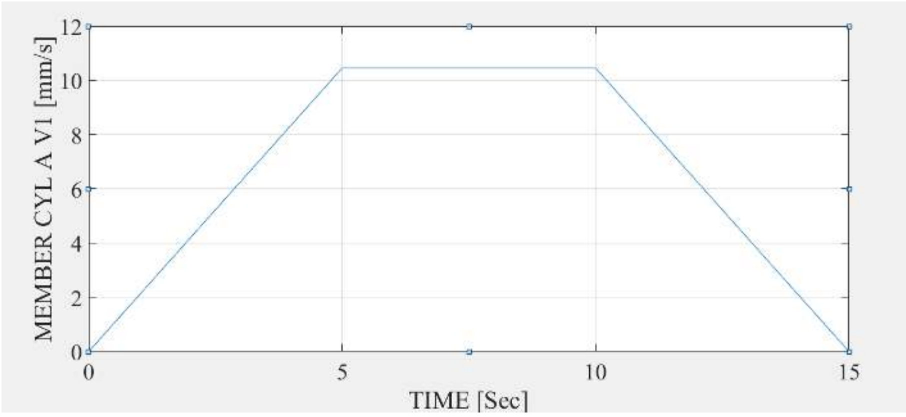

Figure 7.16 Member cyl A velocity profile

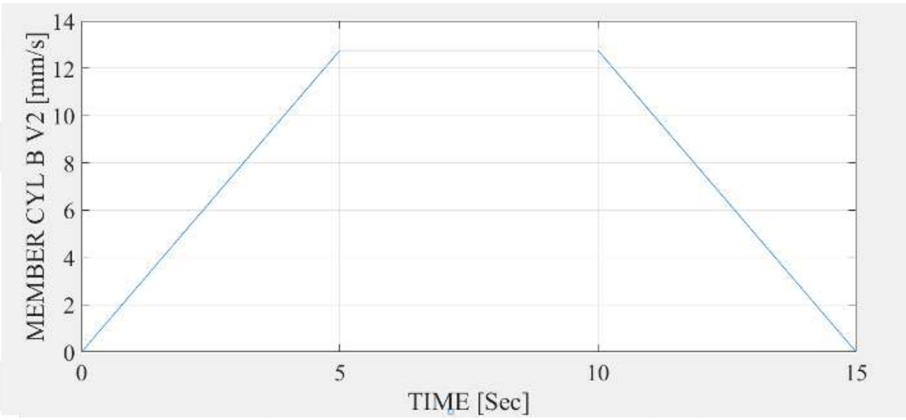

Figure 7.17 Member cyl B velocity profile

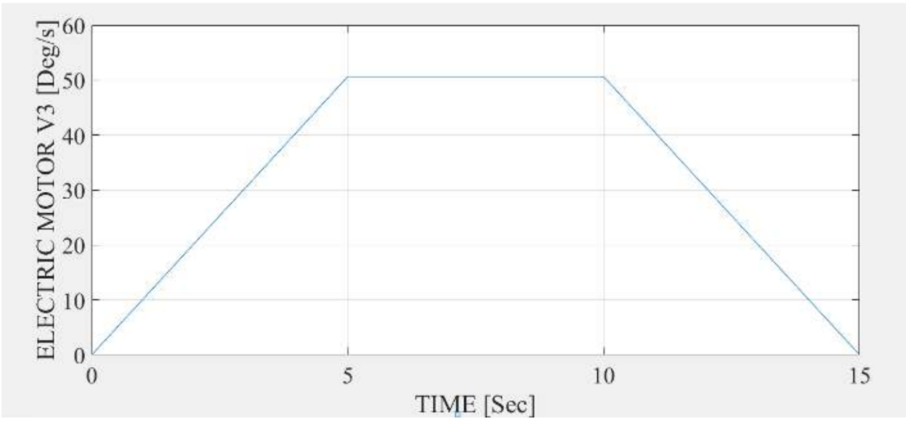

Figure 7.18 Electric motor velocity profile

7.3 Control System

Control system is designed as using feedback linearization method and cartesian model based control algorithm. Position and velocity output is converted to the joint position and velocity as using inverse kinematic and Jacobian method. Output information is compared with the reference position and velocity. Figure 7.19 shows the control system algorithm.

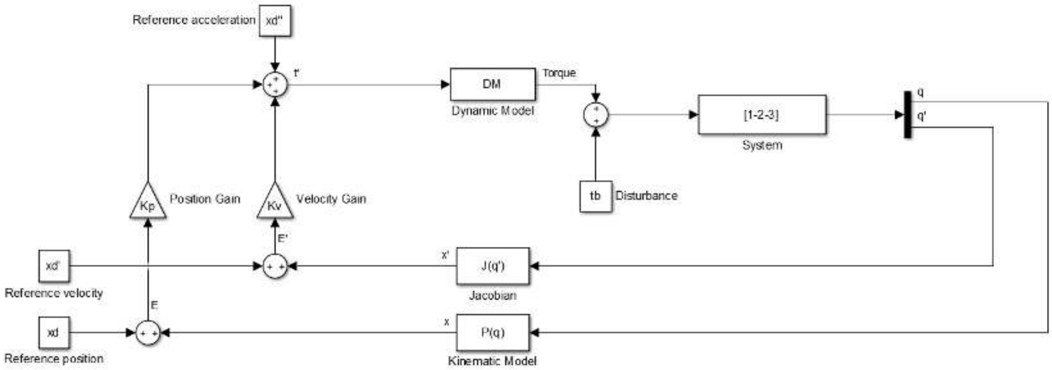

Figure 7.19 Control system

CHAPTER EIGHT
CONCLUSIONS

Three axis welding positioner system can be designed in different multi stage processes which can be respectively described physical and topological structure design, mechanical system design, finite element analysis, kinematic-kinetic analysis and dynamic system modeling, motion planning and time histroy studies.

Firstly, Solidworks program package is used for the mechanical system design and frequency analysis. Also, dynamic analysis studies are handled in the Solidworks Motion module. Also, The program presents simplicity and quick design flexibility to designer in every stage of the design process.

Second, ANSYS Mechanical is used for finite element analysis simulation and the package is suitable for this type of robotic applications. Also the results are obtained after the simulation and the general structure is suitable in the aspect of mechanical strength.

Finally, MATLAB/Simulink is used for the kinematic-kinetic analysis and dynamic modeling of the entire system. Mathematical calculations and iterative kinetic analysis are executed in the program and the resultant graphs are plotted. Also, maximum actuator velocity limits are obtained and hydraulic system is designed.

The three axis welding positioner system is mainly designed welded steel sheet construction and the system has two hydraulic actuators and an electic actuator because of this reason we can describe the system is hybrid manipulator. Kinetic and dynamic calculations are conducted with respect to 1500 kg loading condition and the system is considered for the uniform loading condition.

Different performance tasks are studied, especially weld path 5 is reviewed and maximum actuator speeds are obtained during this welding tasks.

In conclusion, more general design stages and integrated design approaches can be implemented to the system in the design and dynamic analysis phase and performance studies can be multiplied for optimal system design and analysis.

REFERENCES

ABB. (2016*). IRB 1660 ID Six Axis Welding Robot CAD Model.* Retrieved September 28, 2016 from http://new.abb.com/products/robotics/industrial-robots/irb-1660id.

Amindari, A. (2012*). Evaluation of the strength of a three axis serial robot performing a task by integrated dynamic analysis.* M.Sc Thesis, Dokuz Eylül University, İzmir.

Bingül, Z. & Küçük, S. (2015). *Robot kinematiği*. (1st ed.). Kocaeli:Umuttepe Yayınları.

Bingül, Z. & Küçük, S. (2008). *Robot dinamiği ve kontrolü.* İstanbul: Birsen Yayınevi.

Gujarathi, G.P. & Ma, Y.-S. (2011). Parametric cad-cae integration using a common data model. *Journal of Manifacturing Systems, 30,* 118-132.

Harman, T., Dabney, J., & Richert, N.,(2000). *Advanced engineering mathematics with matlab* (2nd ed.). USA: Brooks/Cole.

Hibbeler, R.C. (2009). *Engineering mechanics - dynamics.* (Metric ed.). (A. Soyuçok & O. Soyuçok, trans)

Irco Automation. (2016). *P3X-3 3 Axis Positioner Product Matrix.* Retrieved March 8, 2016 from https://www.ircoautomation.com/products/welding-positioners/3-axis-positioners/

Kaluç, E. & Taban, E. (2004). *İleri kaynak teknolojisi.* Kocaeli:Kocaeli Universitesi.

Karagülle, H., Amindari, A., Akdağ, M., Malgaca, L., & Yavuz, S. (2012). Kinematic – kinetic – rigidity evaluation of a six axis robot performing a task. *International Journal of Advanced Robotic Systems, 9,* 176/2012.

Kim, D.-W., Choi, J.-S. & Nnaji, B. O.(1998). Robot arc welding operations planning with a rotating/tilting positioner. *International Journal of Production Research, 36*, 4, 957-979.

Mrozek, Z. (2003). Computer aided design of mechatronic systems. *International Journal of Applied Mathematics and Computer Science, 13*, 2, 255-267.

Pan, Z., Wang, X., Teng, R. & Cao, X. (2016). Computer-aided design-while-engineering technology in top-down modeling of mechanical product. *Computers in Industry, 75,* 151-161.

Pashkevich, A.P., Dolgui, A.B. & Semkin, K.I. (2003). Kinematic aspects of a robot-positioner system in an arc welding application. *Control Engineering Practice, 11,* 633-647.

Pashkevich, A.P. & Dolgui, A.B. (2006). Kinematic control of a robot-positioner system for arc welding application. *Industrial Robotics: Programming, Simulation and Applications, 3*-86611-286-6, 702.

Sahbaz, H., Karagülle, H. & Malgaca, L.(n.d.) Pc based motion control on an hexapod application, UMTS200, 241-251.

SKF. (2016). *6024 Deep Groove Ball Bearings Product Specsheet.* Retrieved May 28, 2016 from http://www.skf.com/group/products/bearings-units-housings/ball-bearings/deep-groove-ball-bearings/single-row-deep-groove-ball-bearings/deep-groove-ball-bearings/index.html?designation=6024.

Wittler, G. & Moritz, W. (1998). Mechatronic design methods and software in mechanical engineering.(Retrieved March 6,2016)

Wu, J., Gao, J., Li, Song, R., Li, R., Li, Y. & Jiang, L. (2015). The design and control of a 3 dof lower limb rehabilitation robot. *Mechatronics, 33,* 13-22.

Yayla, P. (2001). *Cisimlerin mukavemeti.*(2nd ed.). İstanbul:Caglayan Kitabevi.

Yılmaz Redüktör. (2016). *EV 075 2G80 Motor & Gear Unit.* Retrieved March 19, 2016 from http://www.yr.com.tr/gst/ev/form-a.aspx.